1521-0103/377/1/75–85$35.00
THE JOURNAL OF PHARMACOLOGY AND EXPERIMENTAL THERAPEUTICS

https://doi.org/10.1124/jpet.120.000395
J Pharmacol Exp Ther 377:75–85, April 2021

Increased Interleukin-10 Expression by the Inhibition of Ca^{2+}-Activated K^+ Channel $K_{Ca}3.1$ in $CD4^+CD25^+$ Regulatory T Cells in the Recovery Phase in an Inflammatory Bowel Disease Mouse Model[S]

Susumu Ohya,[1] Miki Matsui,[1] Junko Kajikuri, Kyoko Endo, and Hiroaki Kito

Department of Pharmacology, Graduate School of Medical Sciences, Nagoya City University, Nagoya, Japan

Received October 23, 2020; accepted January 22, 2021

ABSTRACT

Inflammatory bowel diseases (IBD) are chronic inflammatory diseases of the gastrointestinal tract arising from abnormal responses of the innate and adaptative immune systems. Interleukin (IL)-10–producing $CD4^+CD25^+$ regulatory T (T_{reg}) cells play a protective role in the recovery phase of IBD. In the present study, the effects of the administration of the selective Ca^{2+}-activated K^+ channel $K_{Ca}3.1$ inhibitor TRAM-34 on disease activities were examined in chemically induced IBD model mice. IBD disease severity, as assessed by diarrhea, visible fecal blood, inflammation, and crypt damage in the colon, was significantly lower in mice administered 1 mg/kg TRAM-34 than in vehicle-administered mice. Quantitative real-time polymerase chain reaction examinations showed that IL-10 expression levels in the recovery phase were markedly increased by the inhibition of $K_{Ca}3.1$ in mesenteric lymph node (mLN) T_{reg} cells of IBD model mice compared with vehicle-administered mice. Among several positive and negative transcriptional regulators (TRs) for IL-10, three positive TRs—E4BP4, KLF4, and Blimp1—were upregulated by the inhibition of $K_{Ca}3.1$ in the mLN T_{reg} cells of IBD model mice. In mouse peripheral $CD4^+CD25^+$ T_{reg} cells induced by lectin stimulation, IL-10 expression and secretion were enhanced by the treatment with TRAM-34, together with the upregulation of E4BP4, KLF4, and Blimp1. Collectively, the present results demonstrated that the pharmacological inhibition of $K_{Ca}3.1$ decreased IBD symptoms in the IBD model by increasing IL-10 production in peripheral T_{reg} cells and that IL-10^{high} T_{reg} cells produced by the treatment with $K_{Ca}3.1$ inhibitor may contribute to efficient T_{reg} therapy for chronic inflammatory disorders, including IBD.

SIGNIFICANCE STATEMENT

Pharmacological inhibition of Ca^{2+}-activated K^+ channel $K_{Ca}3.1$ increased IL-10 expression in peripheral T_{reg} cells, together with the upregulation of the transcriptional regulators of IL-10: Krüppel-like factor 4, E4 promoter-binding protein 4, and/or B lymphocyte–induced maturation protein 1. The manipulation of IL-10^{high}–producing T_{reg} cells by the pharmacological inhibition of $K_{Ca}3.1$ may be beneficial in the treatment of chronic inflammatory diseases such as inflammatory bowel disease.

Introduction

Inflammatory bowel disease (IBD) is defined as chronic intestinal inflammation with abdominal symptoms such as diarrhea, bloody stools, pain, and vomiting and is prevalent worldwide (Fakhoury et al., 2014). In the United States and Europe, 3 to 4 million individuals have IBD, and its incidence is increasing in several countries in Asia (Kaplan, 2015; Singh et al., 2017). Dextran sodium sulfate (DSS)-induced intestinal inflammation is one of the most widely used nongenetic models of IBD (Eichele and Kharbanda, 2017), and morphologically and symptomatically, it resembles many features of human ulcerative colitis. Acute and chronic models of IBD have been generated by modifying DSS concentrations and administration frequencies with different cytokine profiles (Chassaing et al., 2014). Acute IBD models are used to investigate the roles of cytokines in the induction of IBD symptoms, and chronic models are employed to examine recovery from inflammation (Eichele and Kharbanda, 2017).

This work was supported by a Grant-in-Aid for Scientific Research (C) [16K-8285], a Grant-in-Aid for Fostering Joint International Research (B) [18KK0218] by the Japan Society for the Promotion of Science (JSPS), and a grant from the Bristol-Myers Squibb foundation [53952417].
The authors declare no conflicts of interest associated with this manuscript.
[1]S.O. and M.M. contributed equally to this work.
https://doi.org/10.1124/jpet.120.000395.
[S] This article has supplemental material available at jpet.aspetjournals.org.

ABBREVIATIONS: ACTB, β-actin; AGR2, anterior gradient protein 2 homolog; BATF, basic leucine zipper activating transcription factor–like transcription factor; Blimp, B lymphocyte–induced maturation protein; bp base pair(s) CaMK, Ca^{2+}-dependent calmodulin kinase; CN, calcineurin; Con-A, concanavalin-A; DSS, dextran sodium sulfate; E4BP, E4 promoter-binding protein; ERK, extracellular signal–regulated kinase; Foxp, forkhead box P; HDAC, histone deacetylase; HIF, hypoxia-inducible factor; IBD, inflammatory bowel disease; IFN, interferon; IL, interleukin; JAK, Janus kinase; K_{Ca}, Ca^{2+}-activated K^+ (channel); KLF, Krüppel-like factor; MAPK, mitogen-activated protein kinase; mLN, mesenteric lymph node; NFAT, nuclear factor of activated T cells; P-, phospho-; PCR, polymerase chain reaction; PI3K, phosphoinositide 3-kinase; RoR, retinoic acid receptor–related orphan receptor; STAT, signal transducer and activator of transcription; Th helper T (cell) TR, transcriptional regulator; T_{reg}, regulatory T (cell); TRIM, tripartite motif containing.

In the recovery phase, a reduction in disease activity is accompanied by the increased production of anti-inflammatory mediators such as interleukin (IL)-10.

IL-10 is the most important anti-inflammatory cytokine in the immune system, and it is produced by lymphocytes, macrophages, mast cells, and dendritic cells (Ng et al., 2013). Therefore, IL-10 is protective against a number of autoimmune responses, such as rheumatoid arthritis. IL-10–secreting $CD4^+CD25^+$ regulatory T (T_{reg}) cells in mesenteric lymph nodes (mLN) and the lamina propria are essential for the maintenance of intestinal homeostasis and exert protective effects during the disease process of IBD. Low levels of IL-10 increase disease severity in chronic IBD, and IL-10–deficient mice exhibit severe IBD symptoms (Kennedy et al., 2000; Shah et al., 2012). IL-10 levels have been shown to markedly increase in the recovery phase of the DSS-induced IBD model but not in the induction phase, together with the expression levels of the T_{reg} characteristic markers CD25 and Foxp3 (Bento et al., 2012). Therefore, IL-10 supplementation and T_{reg} therapy are therapeutic regimens for the prevention of autoimmunity, including IBD. Many IL-10 transcriptional regulators (TRs) with/without the transactivation of promoters have been identified in different cell types, including T cells (Rutz and Ouyang, 2016), and some are activated by the JAK/STAT3, PI3K/AKT, MAPK/ERK, and CN-NFAT signaling pathways (Martin et al., 2003; Bouhamdan et al., 2015). A member of the legume lectin family, concanavalin-A (Con-A), is a well known T-cell mitogen that promotes differentiation into IL-10–producing $CD4^+CD25^+Foxp3^+$ T_{reg} cells (Shanmugasundaram and Selvaraj, 2011) and is used as an efficient tool for investigating the characteristics of thymic and peripherally induced T_{reg} cells in vitro.

The intermediate-conductance Ca^{2+}-activated K^+ channel $K_{Ca}3.1$ is involved in the pathogenesis of IBD (Di et al., 2010; Ohya et al., 2014). In the $CD4^+CD25^-$ T cells of DSS-induced acute IBD model mice, the upregulation of $K_{Ca}3.1$ via epigenetic modifications enhanced the expression and production of the proinflammatory cytokine interferon (IFN)-γ (Ohya et al., 2014; Matsui et al., 2018), suggesting that the inhibition of $K_{Ca}3.1$ is useful for targeting inflammatory $CD4^+$ cells in autoimmune diseases, including IBD. However, the functional role of $K_{Ca}3.1$ in T_{reg} cells in the recovery phase from IBD symptoms remains unclear. In human T-cell lymphoma HuT-78 cells, a $K_{Ca}3.1$ activator repressed the expression levels of IL-10 by preventing SMAD2 phosphorylation and its nuclear translocation (Matsui et al., 2019).

In the present study, we examined the in vivo effects of the inhibition of $K_{Ca}3.1$ on IL-10 expression in mLN T_{reg} cells in the recovery phase from inflammation using IBD model mice established by Sha et al. (2013). The inhibition of $K_{Ca}3.1$ also exerted similar effects on IL-10 expression and secretion in peripheral T_{reg} cells induced in vitro by the Con-A stimulation, and the underlying mechanisms were examined to facilitate the development of T_{reg} therapies for IBD.

Materials and Methods

DSS-Induced Mouse IBD Model. Female C57BL/6J (7 to 8 weeks of age) mice were obtained from Japan SLC (Shizuoka, Japan). They were given distilled water containing 2.5% (w/v) DSS (molecular weight 36–50 kDa) (MP Biomedicals, Santa Ana, CA) ad libitum for 7 days followed by 5 days of normal drinking water (Sha et al., 2013) (Fig. 1A). Control mice were given drinking water only. The clinical assessment of inflammation included the daily monitoring of weight loss. Mice were euthanized 12 days later, tissue samples were collected, and colitis and inflammation were macroscopically assessed according to our previous study (Ohya et al., 2014). The macroscopic appearance of stool consistency (diarrhea) and visible fecal blood were scored separately on a scale of 0–3 (Ohya et al., 2014). Two subcutaneous injections (on days 5 and 9) of TRAM-34 (1 mg/kg) were given in the loose skin around the neck, and the injection volume was 50 μl each time. The same volume of DMSO was administered to the "vehicle" group. All experiments were performed in accordance with the guiding principles for the care and use of laboratory animals in Nagoya City University and also with the approval of the president of Nagoya City University (H29M-50).

Histologic Scoring. The damaged portion of the colon in IBD model mice was confirmed by Alcian staining as previously reported (Ohya et al., 2014). Regarding histologic assessments, a 1-cm tissue sample of the range from colon was fixed in 10% buffered formalin, embedded in a paraffin block, cut into 5-μm-thick sections, and stained with hematoxylin and eosin. Inflammation scores were determined as the multiplication of the grade of inflammation severity (grade 0–3) and its extent (grade 0–3) (Dieleman et al., 1998; Ohya et al., 2014). Data were obtained from three sections of the colon measured at least 200 μm apart per animal.

Isolation of $CD4^+CD25^+$ T_{reg} Cell Subsets. $CD4^+CD25^+$ T_{reg} cell subsets were isolated from mice mLN and spleen cell suspensions by Dynabeads FlowComp Mouse $CD4^+CD25^+$ Treg Cells according to the experimental protocol supplied by Thermo Fisher Scientific (Waltham, MA) (Nakakura et al., 2015). A flow cytometric analysis [FACSCanto II flow cytometers (BD Biosciences, San Jose, CA)] using antibodies labeled with different fluorophores (fluorescein isothiocyanate-CD4 and phycoerythrin-CD25) confirmed that 90% of purified T cells were $CD4^+CD25^+$.

Real-Time PCR. Total RNA extraction and cDNA synthesis from $CD4^+CD25^+$ T cells were performed as previously reported (Matsui et al., 2018). The resulting cDNA products were amplified with gene-specific primers, which were designed using Primer Express software (version 1.5; Applied Biosystems, Foster city, CA). Real-time PCR was performed using SYBR Premix Ex Taq II (TaKaRa BIO, Osaka, Japan) on ABI 7500 real-time PCR instruments (Applied Biosystems) (Matsui et al., 2018). The following PCR primers were used: $K_{Ca}3.1$ (GenBank accession number: NM_008433, 343–452), 110 bp; IL-10 (NM_010548, 245–355), 111 bp; IL-17A (NM_010552, 165–277), 113 bp; IL-17F (NM_141856, 185–304), 120 bp; IFN-γ (NM_008337, 222–323), 102 bp; CD25 (NM_008367, 522–642), 121 bp; Foxp3 (NM_001199347, 823–942), 120 bp; nucleoside diphosphate kinase (NDPK)-B (NM_008705, 467–597), 131 bp; PI3K-C2B (NM_001099276, 2293–2422), 130 bp; phosphohistidine phosphatase (PHPT)-1 (NM_029293, 69–189), 121 bp; myotubularin-related protein (MTMR)-6 (NM_144843, 722–832), 111 bp; HDAC2 (NM_008229, 1436–1546), 111 bp; HDAC3 (NM_010411, 1106–1226), 121 bp; E4BP4 (NM_017373, 1434–1554), 121 bp; cMAF (NM_001025577, 964–1083), 120 bp; GATA3 (NM_008091, 1366–1485), 120 bp; AGR2 (NM_011783, 342–461), 120 bp; IL-27 (NM_145636, 456–577), 122 bp; Blimp1 (NM_001198, 434–553), 120 bp; KLF4 (NM_010637, 1796–1915), 120 bp; RoRα (NM_013646, 1263–1382), 120 bp; RoRγt (AF163668, 794–913), 120 bp; Runt-related transcription factor 1 (RUNX1) (NM_001111021, 1019–1138), 120 bp; HIF-1α (NM_010431, 963–1062), 100 bp; TRIM33 (NM_053170, 3123–3242), 120 bp; SMAD2 (NM_010754, 666–785), 120 bp; BATF (NM_016767, 301–423), 121 bp; interferon regulatory factor 4 (NM_013674, 620–739), 120 bp; STAT3 (NM_213659, 707–826), 120 bp; JunB (NM_008416, 1169–1309), 141 bp; and β-actin (ACTB) (NM_031144, 419–519), 101 bp. Unknown quantities relative to the standard curve for a particular set of primers were calculated (Matsui et al., 2018), yielding the transcriptional quantitation of gene products relative to ACTB.

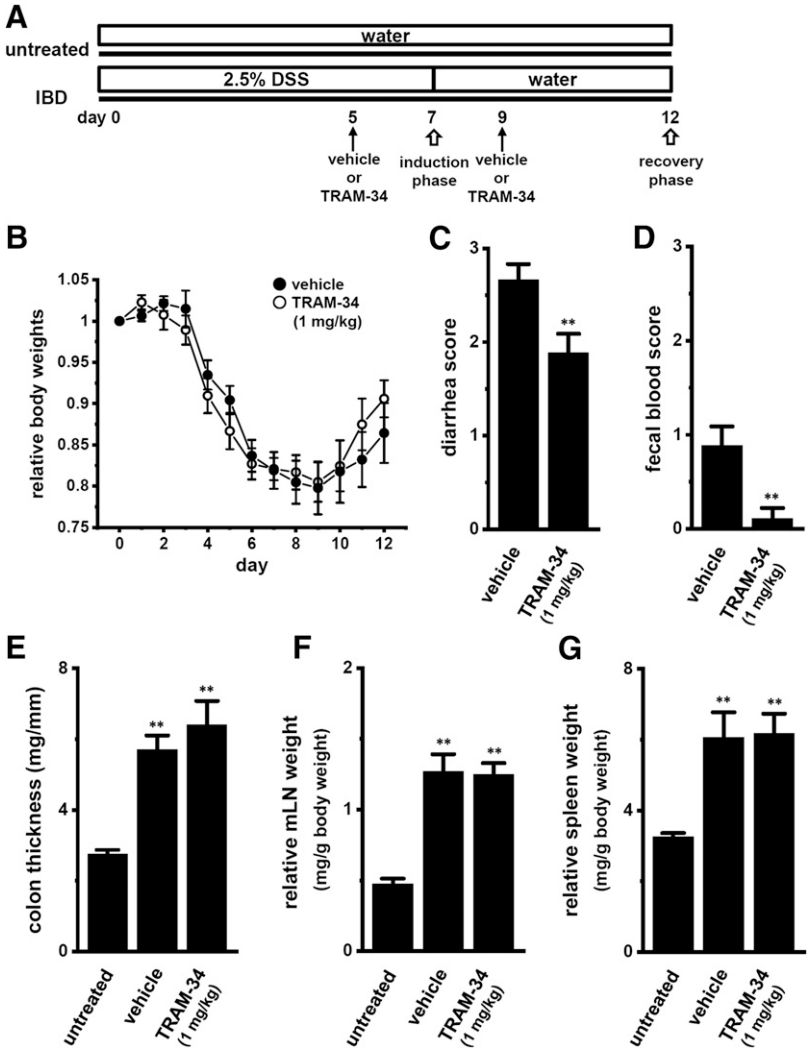

Fig. 1. Effects of the administration of TRAM-34 (1 mg/kg, s.c.) on the clinical assessment (body weight, diarrhea, and bloody feces), colonic inflammation, and lymphoid tissue weights in IBD model mice. (A) Experimental protocol for IBD induction in mice. The IBD model was prepared by the administration of 2.5% DSS in drinking water for 7 days (day 7, induction phase) and distilled water for the following 5 days (day 12, recovery phase). (B) Time course of DSS-induced body weight loss in IBD model mice administered vehicle (closed circles) or TRAM-34 (1 mg/kg) (open circles). Body weight prior to DSS treatment (day 0) was expressed as 1.0. (C and D) Therapeutic effects of repeated administration of TRAM-34 (1 mg/kg, s.c.) on diarrhea (C) and visible fecal blood (D) scores in the recovery phase of IBD model mice. (E) The colon weight/length ratio was measured in untreated mice and vehicle- and TRAM-34–administered IBD model mice. (F and G) mLN and spleen weights (in milligrams) were measured in untreated mice and vehicle- and TRAM-34–administered IBD model mice and expressed as a ratio to body weight (in grams). Results were expressed as means ± S.E.M. ($n = 9$ for each). $^{**}P < 0.01$ vs. the vehicle control (C and D) or untreated mice (E–G).

Preparation of $CD4^+CD25^+$ T_{reg} Cells Induced In Vitro by Concanavalin-A Stimulation. Cell suspensions were prepared by pressing the spleens of female C57BL/6J (8 to 9 weeks of age) mice with frosted slide glasses in RPMI 1640 medium (FUJIFILM Wako Pure Chemicals, Osaka, Japan) supplemented with 10% heat-inactivated fetal calf serum (Sigma, St. Louis, MO) and antibiotics (penicillin and streptomycin; FUJIFILM Wako Pure Chemicals). Splenocytes were prepared by red blood cell lysis. Isolated splenocytes were cultivated in RPMI 1640 medium supplemented with Con-A (5 μg/ml) and IL-2 (10 U/ml) for 48 hours. Various concentrations of TRAM-34 (0, 1, and 10 μM) were added. At 24 hours later, the supernatant and cells were recovered for ELISA, real-time PCR, and Western blot analyses.

Measurement of IL-10 and IL-17A Production by ELISA. Mouse IL-10 and IL-17A levels in culture supernatant samples were measured with IL-10 and IL-17A Mouse ELISA kits, respectively (Thermo Fisher Scientific), according to the experimental protocol.

Western Blotting. Protein lysates were prepared from mouse splenic $CD4^+CD25^+$ T cells using radioimmunoprecipitation assay (RIPA) lysis buffer. After the protein quantification using the DC protein assay (Bio-Rad Laboratories, Hercules, CA), protein lysates were subjected to SDS-PAGE (10%). Blots were incubated with anti–phospho-Smad2 (Ser465/467) (P-Smad2), anti–phospho-Smad3 (Ser423/425) (P-Smad3) (Cell Signaling Technology Japan, Tokyo, Japan), anti–phospho-AKT (Ser473) (P-AKT) (BioLegend, San Diego, CA), anti–phospho-STAT3 (Tyr705) (P-STAT3) (BioLegend), anti–phospho-ERK1 (Thr202/Tyr204)/ERK2 (Thr185/Tyr187) (P-ERK1/2) (R&D Systems, Minneapolis, MN), and anti-ACTB (Medical & Biologic Laboratories, Nagoya, Japan) antibodies. After staining with anti-rabbit horseradish peroxidase–conjugated IgG (Merck, Darmstadt, Germany), an enhanced chemiluminescence detection system (Nacalai Tesque, Kyoto, Japan) was used to detect the bound antibody. The images were visualized and analyzed using Amersham Imager 600 (GE Healthcare Japan, Tokyo, Japan). The light intensities of band signals were digitalized using ImageJ software (version 1.42; National Institutes of Health, Bethesda, MD). Relative protein expression levels in the control were expressed as 1.0.

Cellular Distribution of P-Smad2 and P-Smad3. Mouse splenic $CD4^+CD25^+$ T cells were fixed and permeabilized, and then cells were stained by anti–P-Smad2 and anti–P-Smad3 antibodies labeled with an Alexa Fluor 488–conjugated secondary antibody (Abcam, Cambridge, UK) and 4′,6-diamidino-2-phenylindole for nucleic acid staining (Matsui et al., 2019). Fluorescence images were visualized using a confocal laser scanning microscope system (A1R; Nikon, Tokyo, Japan).

Chemicals. TRAM-34 was purchased from Santa Cruz Biotechnology (Dallas, TX); KN-62 was from Medchemexpress (Monmouth Junction, NJ); ciclosporin A was from FUJIFILM Wako Pure Chemicals; 5,15-diphenylporphyrin was from Abcam (Cambridge, UK); and AZD5363, everolimus, LY364947, and SCH772984 were from Cayman

Chemical (Ann Arbor, MI). All other chemicals used in the present study were from Sigma-Aldrich, FUJIFILM Wako Pure Chemicals, or Nacalai Tesque unless otherwise stated.

Statistical Analysis. Statistical analyses were performed with the statistical software XLSTAT. To assess the significance of differences between two groups and among multiple groups, the unpaired/paired Student's t test with Welch's correction or Tukey's test was used. Data that were not normally distributed were analyzed using Mann-Whitney's U test. Results with a P value of less than 0.05 or 0.01 were considered to be significant. Data are presented as means ± S.E.M.

Results

Effects of the Subcutaneous Administration of the $K_{Ca}3.1$ Blocker TRAM-34 on IBD Symptoms in DSS-Induced IBD Model Mice. In the IBD model, loose and bloody feces were observed 3 days after exposure to 2.5% DSS in drinking water. A previous study reported that the plasma concentration of TRAM-34 was more than 10-fold higher than the in vitro IC_{50}, even 4 days after the single subcutaneous administration of 1 mg/kg TRAM-34 (Ohya et al., 2014). In the present study, to investigate the therapeutic effects of $K_{Ca}3.1$ inhibition, TRAM-34 was administered twice on days 5 and 9 (Fig. 1A). At 12 days after the exposure to 2.5% DSS for 7 days followed by 5 days of normal water, the effects of the repeated administration of TRAM-34 on macroscopic (body weight change, diarrhea and visible fecal blood, colon thickening) and microscopic (crypt damage and colonic inflammation) IBD symptoms were assessed as previously reported (Ohya et al., 2014; Nakakura et al., 2015). Figure 1B showed the changes in body weight during the induction and recovery phases in vehicle- and TRAM-34–administered (closed circles and open circles, respectively) IBD model mice (n = 9 for each). By drinking water for 5 days (from days 8 to 12), body weight loss was partially recovered. The recovery rate of body weight loss was relatively large in TRAM-34–administered mice compared with vehicle-administered mice; however, no significant differences were found between both groups (Fig. 1B). In vehicle-administered IBD model mice, the average scores of diarrhea and visible fecal blood on day 12 were 2.67 ± 0.17 and 0.89 ± 0.20 (n = 9 for each), respectively, and the fecal blood score was lower than that on day 7 (2.83 ± 0.17, n = 6). In IBD model mice, both scores were significantly reduced by the inhibition of $K_{Ca}3.1$: 1.89 ± 0.20 (P = 0.0092) and 0.11 ± 0.11 (P = 0.0054) (n = 9 for each), respectively (Fig. 1, C and D). The colon was thicker and the mice mLN and spleen were larger in vehicle-administered IBD model mice than in untreated mice, and they were not affected by the inhibition of $K_{Ca}3.1$ (Fig. 1, E–G) because of the decrease in these parameters on day 12 compared with those on day 7: 1.52 ± 0.12, 7.16 ± 0.56 mg/g and 7.92 ± 0.38 mg/mm (n = 8 for each) in mLN weight, spleen weight, and colon thickness. Colonic inflammation and crypt damage were assessed by histologic visualization (Fig. 2, A–C) and scoring (Fig. 2, D and E). In vehicle-administered IBD model mice, average scores were 15.33 ± 0.73 and 14.56 ± 0.67 (n = 9 for each), respectively. Both scores were significantly reduced by the inhibition of $K_{Ca}3.1$: 11.33 ± 1.01 (P = 0.0058) and 9.78 ± 0.78 (P = 0.0002) (n = 9 for each), respectively (Fig. 2, D and E). Preliminarily, we examined the effects of subcutaneous administration of 0.1 mg/kg TRAM-34 on the scores of diarrhea and visible fecal blood. No significant improvement in IBD symptoms was found after administration of 0.1 mg/kg TRAM-34. Unexpectedly, improvement of IBD symptoms was not observed after administration of 10 mg/kg TRAM-34. In 10 mg/kg TRAM-34–administered IBD model mice, the average scores of diarrhea and visible fecal blood were 2.78 ± 0.15 and 0.78 ± 0.15 (n = 9 for each), respectively, and no significant changes were found between vehicle- and 10 mg/kg TRAM-34–administered groups (P = 0.1732 and 0.3861, respectively) (Supplemental Fig. 1, A and B). Also, in 10 mg/kg TRAM-34–administered IBD model mice, the average scores of colonic inflammation and crypt damage were 15.44 ± 1.02 and 15.11 ± 0.81 (n = 9 for each), respectively, and no significant changes were found between vehicle- and 10 mg/kg TRAM-34–administered groups (P = 0.2046 and 0.1229, respectively) (Supplemental Fig. 1, C and D). A recent study by Süss et al. (2020) suggested that $K_{Ca}3.1$ may have a protective role in epithelial barrier in IBD. Therefore, the administration of 10 mg/kg TRAM-34 may deteriorate IBD symptoms by dysregulating epithelial barrier function. In untreated mice, the administration of 1 mg/kg TRAM-34 on days 5 and 9 did not affect any IBD symptoms (body weight loss, colon thickening, diarrhea, and visible fecal blood) (n = 6). In mLN $CD4^+CD25^-$ T cells, the expression levels of proinflammatory cytokines (IFN-γ and IL-17F) were significantly increased in the induction phase; however, they are recovered to basal levels in the recovery phase, and no significant changes in them were found by the administration of 1 mg/kg TRAM-34 (Supplemental Fig. 2).

Increased IL-10 Expression by TRAM-34 Administration in mLN $CD4^+CD25^+$ T_{reg} Cells of IBD Model Mice. Bento et al. (2012) showed that IL-10 expression was markedly increased in inflamed colon segments in the recovery phase in the DSS-induced IBD model ("recovery phase") but not in the inflammation induction phase ("induction phase"). Our preliminary experiments also showed the upregulation of IL-10 and T_{reg} cell markers (CD25 and Foxp3) in mLN at the end of the recovery phase (day 12) and no changes in the induction phase (day 7) (Supplemental Fig. 3). A fluorescent dual color dot plot of fluorescein isothiocyanate-CD4 versus phycoerythrin-CD25 was analyzed in living mLN cells using flow cytometry. The percentage of the $CD4^+CD25^+$ subset within the whole $CD4^+$ T-cell population in the mLN was significantly higher in IBD model mice than in untreated mice (n = 4 for each, P = 0.0046) (Supplemental Fig. 4A); however, no significant changes were observed in the mLN of TRAM-34–administered IBD model mice (Supplemental Fig. 4B). Furthermore, no significant differences were observed in the expression levels of CD25 transcripts in mLN T_{reg} cells between vehicle- and TRAM-34–administered IBD model mice (Supplemental Fig. 4C).

No significant changes were observed in the expression levels of IL-10 transcripts in mLN $CD4^+CD25^+$ T_{reg} cells in the induction phase in IBD model mice (n = 4 for each) (Fig. 3A); however, significant increases in the expression levels of IL-10 transcripts were noted in the recovery phase (n = 4 for each, P = 0.0006) (Fig. 3B). An approximately 5-fold increase in the expression levels of IL-10 transcripts was observed in these mice after the administration of TRAM-34: 0.049 ± 0.006 and 0.254 ± 0.052 (in arbitrary units) in the vehicle- and TRAM-34–administered groups, respectively (n = 5 for each, P = 0.006) (Fig. 3C).

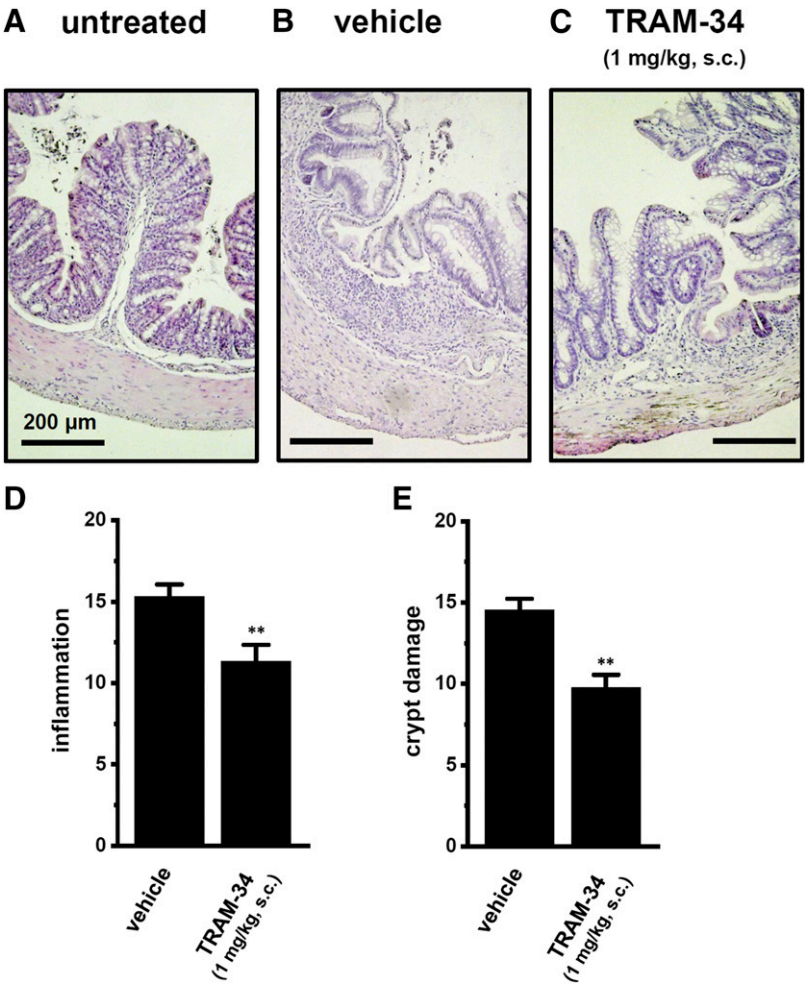

Fig. 2. Effects of the subcutaneous administration of TRAM-34 (1 mg/kg, s.c.) on colonic inflammation in IBD model mice. (A–C) Photographs of colon sections from untreated (A) and IBD model mice administered vehicle (B) or TRAM-34 (1 mg/kg) (C) with hematoxylin and eosin (magnification, 100×). Scale bars, 200 μm. (D and E) Colon damage was assessed histologically by inflammation and crypt damage scores. Results are expressed as means ± S.E.M. (n = 9). $^{**}P < 0.01$ vs. vehicle-administered mice.

We previously reported the increased expression of $K_{Ca}3.1$ in the $CD4^+CD25^-$ T cells of acute IBD model mice (Ohya et al., 2014). We investigated the expression levels of $K_{Ca}3.1$ and its regulatory molecules in mLN T_{reg} cells during the recovery phase in IBD model mice. No significant changes were observed in the expression levels of $K_{Ca}3.1$ in T_{reg} cells in the recovery phase between IBD model and untreated mice (n = 4 for each) (Supplemental Fig. 5A). Matsui et al. (2018) showed that the inflammation-associated upregulation of the histone deacetylases HDAC2 and HDAC3 enhanced $K_{Ca}3.1$ transcription in the inflammatory $CD4^+CD25^-$ T cells of acute IBD model mice. However, in the recovery phase in IBD model mice, no significant changes were found in the expression levels of their transcripts (n = 4 for each) (Supplemental Fig. 5, B and C). Additionally, no significant changes were noted in the expression levels of the positive and negative regulators of $K_{Ca}3.1$ (NDPK-B, PI3K-C2B, PHPT-1, and MTMR-6) in T_{reg} cells in the recovery phase in IBD model mice (Supplemental Fig. 5, D–G). Hypoxia is involved in intestinal inflammation in patients with IBD (Westendorf et al., 2017), and the activation of HIF-1α has been shown to promote T_{reg} activity (Colgan and Taylor, 2010). The inflammation-associated induction of HIF-1α expression was observed in T_{reg} cells in IBD model mice (n = 4 for each, P = 0.0088) (Fig. 4D).

Molecular Identification of Possible TRs Contributing to the Upregulation of IL-10 by the Inhibition of $K_{Ca}3.1$ in mLN T_{reg} Cells of IBD Model Mice. A number of positive and negative TRs of IL-10 have been detected in lymphoid and myeloid cell subsets, including T_{reg} cells (Neumann et al., 2019). To identify the TRs potentially contributing to the $K_{Ca}3.1$ inhibition–induced upregulation of IL-10 in the mLN T_{reg} cells of IBD model mice, the transcriptional expression levels of 13 candidates (Foxp3, cMAF, E4BP4, KLF4, TRIM33, RoRγt, BATF, GATA3, AGR2, Blimp1, IL-27, JunB, and HIF-1α) (Rutz and Ouyang, 2016; Neumann et al., 2019) were assessed by real-time PCR. As shown in Supplemental Fig. 6, A, C–E, no significant differences were observed in the expression levels of four candidates (Foxp3, RoRγt, BATF, and GATA3) between the T_{reg} cells of the vehicle- and TRAM-34–administered groups (n = 5 for each), and AGR2, IL-27, and JunB were rarely expressed (under 0.002 in arbitrary units) in both groups. Consistent with the upregulation of IL-10, the expression of the three positive TRs, E4BP4, KLF4, and Blimp1, was increased by the inhibition of $K_{Ca}3.1$ in the mLN T_{reg} cells of IBD model mice (n = 5 for each, P = 0.0023, 0.0000, and 0.0000, respectively) (Fig. 4, E–G). A negative correlation was observed between changes in the expression levels of positive TRs (cMAF, HIF-1α) and negative TR (TRIM33) (n = 5 for each, P = 0.0011, 0.0433, and 0.0000 in cMAF, HIF-1α, and TRIM33, respectively) (Fig. 4H; Supplemental Fig. 6, B and F). The expression levels of E4BP4 and KLF4, but not Blimp1, were significantly higher in T_{reg} cells in the recovery phase than in those from untreated mice (n = 4 for each, P = 0.0006 and 0.0001 in E4BP4 and KLF4, respectively) (Fig. 4, A–C).

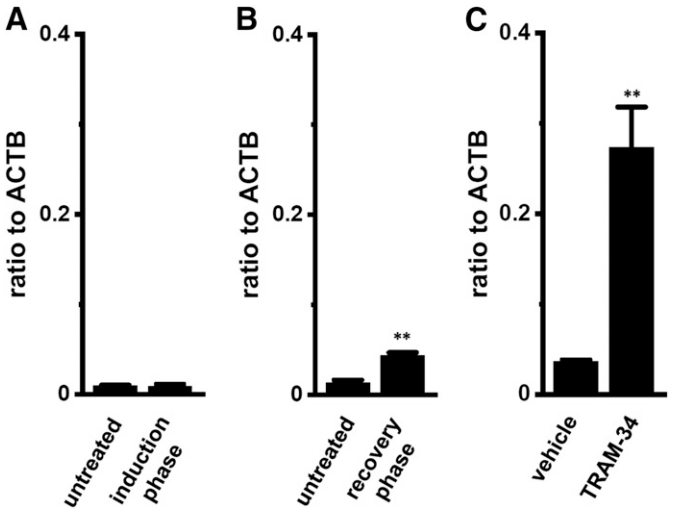

Fig. 3. Increased IL-10 expression by the administration of TRAM-34 (1 mg/kg, s.c.) in mLN $CD4^+CD25^+$ T_{reg} cells in the recovery phase in IBD model mice. (A–C) Real-time PCR examinations for the transcriptional expression of IL-10 in the mLN T_{reg} cells of untreated and IBD model mice in the induction phase (n = 4 for each) (A), of untreated mice and IBD model mice in the recovery phase (n = 4 for each) (B), and of IBD model mice administered vehicle and TRAM-34 (1 mg/kg) in vivo (n = 5 for each) (C). Expression levels were expressed as a ratio to ACTB. Results are expressed as means ± S.E.M. $^{**}P < 0.01$ vs. untreated mice (B) or vehicle-administered mice (C).

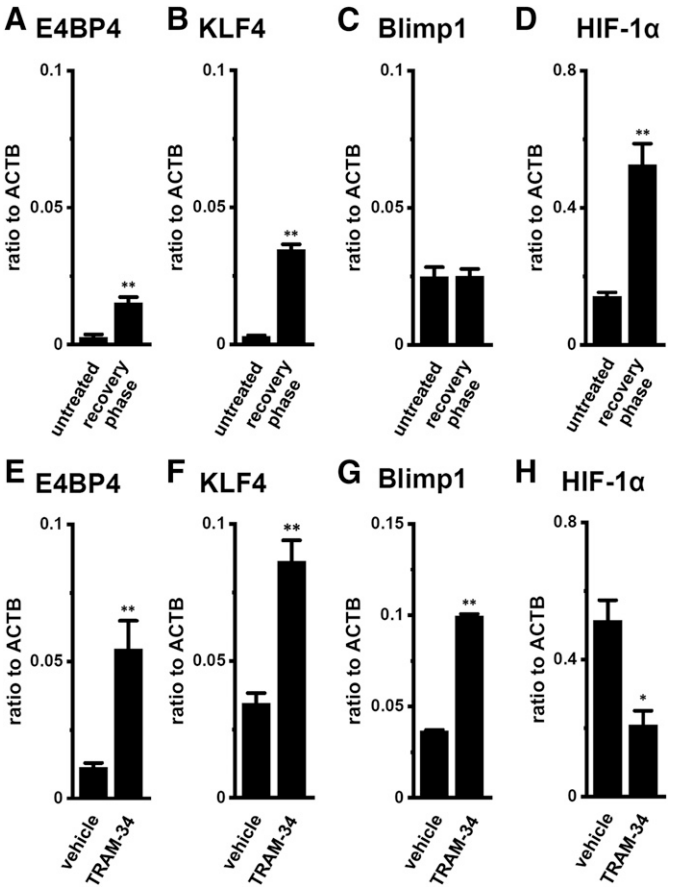

Fig. 4. Expression levels of transcriptional regulators (E4BP4, KLF4, Blimp1, and HIF-1α) for IL-10 by the administration of TRAM-34 (1 mg/kg, s.c.) in mLN $CD4^+CD25^+$ T_{reg} cells in the recovery phase in IBD model mice. (A–H) Real-time PCR examinations for the transcriptional expression of E4BP4 (A and E), KLF4 (B and F), Blimp1 (C and G), and HIF-1α (D and H) in mLN T_{reg} cells in untreated mice and the recovery phase in IBD model mice (A–D) and in the recovery phase in IBD model mice administered vehicle and TRAM-34 (1 mg/kg) in vivo (E–H) (n = 4 for each). Expression levels were expressed as a ratio to ACTB. Results are expressed as means ± S.E.M. *, $^{**}P < 0.05$, 0.01 vs. untreated mice or vehicle-administered mice.

Therefore, the activation of E4BP4 and/or KLF4 may be the mechanism underlying the $K_{Ca}3.1$ inhibition–induced upregulation of IL-10 in the peripheral T_{reg} cells of IBD model mice.

Upregulation of IL-17A by the Administration of TRAM-34 in mLN $CD4^+CD25^+$ T_{reg} Cells of IBD Model Mice. Increased numbers of IL-17A–producing $CD4^+CD25^+Foxp3^+$ T_{reg} cells, which are protective against IBD, have been reported in patients with IBD (Li and Boussiotis, 2013) and a chronic IBD mouse model (Hovhannisyan et al., 2011). In the present study, increased expression levels of IL-17A transcripts in mLN T_{reg} cells were detected in the recovery phase in IBD model mice (n = 4 for each, P = 0.0096) (Fig. 5B) but not in the induction phase (Fig. 5A) (n = 4 for each). Similar to the marked increase observed in IL-10 expression levels, an approximately 6-fold increase in the expression levels of IL-17A transcripts was noted after the administration of TRAM-34: 0.005 ± 0.002 and 0.027 ± 0.006 (in arbitrary units) in vehicle- and TRAM-34–administered IBD model mice, respectively (n = 5 for each, P = 0.0028) (Fig. 5C).

Six candidates, cMAF, KLF4, RoRγt, BATF, HIF-1α, and GATA3, are common positive TRs of IL-10 (Capone and Volpe, 2020). TRIM33 is a positive TR of IL-17A, in contrast to IL-10 (Tanaka et al., 2018). No significant differences were observed in the expression levels of other IL-17A TRs, RoRα, RUNX1, STAT3, interferon regulatory factor 4, and SMAD2, between the two groups (Supplemental Fig. 7). The expression levels of the two positive TRs of IL-17A, KLF4 and TRIM33, were significantly increased by the inhibition of $K_{Ca}3.1$ in the mLN T_{reg} cells of IBD model mice (Fig. 4F; Supplementary Fig. 6F). These results suggested that the activation of KLF4 and/or TRIM33 is the underlying mechanism of the $K_{Ca}3.1$ inhibition–induced upregulation of IL-17A in the peripheral T_{reg} cells of IBD model mice.

Effects of the Inhibition of $K_{Ca}3.1$ In Vitro on IL-10 and IL-17A Transcription and Production in Mouse Peripheral $CD4^+CD25^+$ T_{reg} Cells Differentiated by Con-A Stimulation. To directly examine the effects of the inhibition of $K_{Ca}3.1$ on IL-10/IL-17A expression and secretion in peripherally induced T_{reg} cells, we used the Con-A–differentiated splenic $CD4^+CD25^+$ T_{reg} cells of mice. We previously reported that the ratio of the $CD4^+CD25^+$ T-cell population relative to that of $CD4^+$ T cells was increased by more than 5-fold (approximately 55%) by Con-A stimulation for 48 hours (Tagishi et al., 2016). As shown in Fig. 6, A and B, IL-10 transcription and secretion in T_{reg} cells were both increased by the treatment with 10 μM TRAM-34 for 24 hours (n = 4 for each). IL-10 secretion was increased approximately 1.5-fold by the inhibition of $K_{Ca}3.1$ for 24 hours in T_{reg} cells (Fig. 6B). Similarly, IL-17A transcription and secretion were increased by the treatment with TRAM-34 for 24 hours (n = 4 for each) (Fig. 6C, D). IL-17A secretion was increased approximately 1.4-fold by the inhibition of $K_{Ca}3.1$ for 24 hours in T_{reg} cells (Fig. 6D). Consistent with the results obtained on the in vivo effects of the administration of TRAM-34 on IL-10 and/or IL-17A TRs in the mLN T_{reg} cells of IBD model mice, the transcription of E4BP4, KLF4, TRIM33, and Blimp1

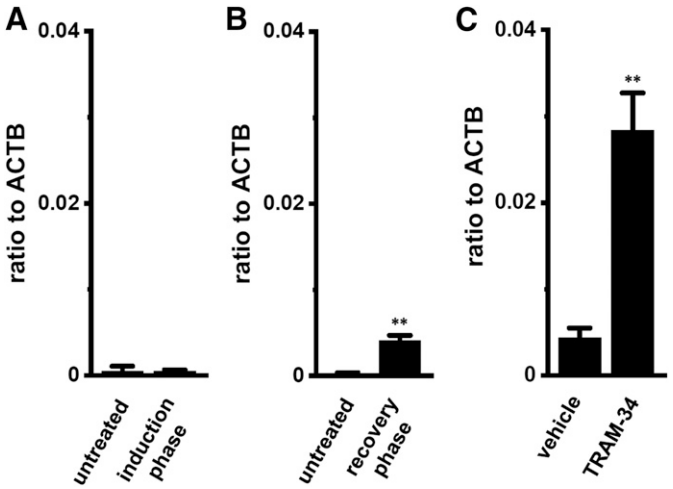

Fig. 5. Increased IL-17A expression in mLN $CD4^+CD25^+$ T_{reg} cells in the recovery phase in IBD model mice after administration of TRAM-34 (1 mg/kg, s.c.). (A–C) Real-time PCR examinations for the transcriptional expression of IL-17A in the mLN T_{reg} cells of untreated and IBD model mice in the induction phase (n = 4 for each) (A), of untreated mice and IBD model mice in the recovery phase (n = 4 for each) (B), and of IBD model mice administered vehicle and TRAM-34 (1 mg/kg) in vivo (n = 5 for each) (C). Expression levels were expressed as a ratio to ACTB. Results are expressed as means ± S.E.M. $^{**}P < 0.01$ vs. untreated mice (B) or vehicle-administered mice (C).

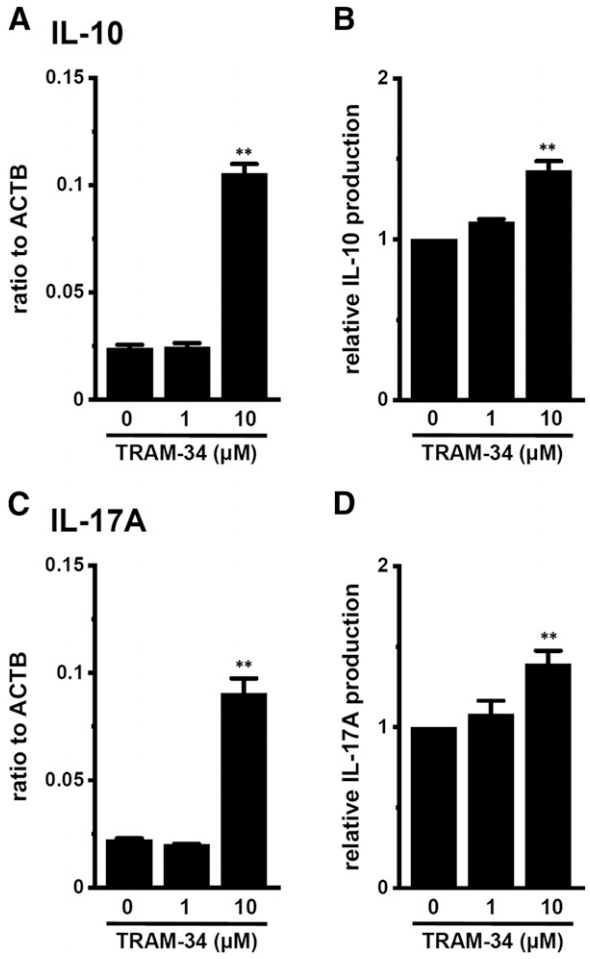

Fig. 6. Increased IL-10 and IL-17A expression and secretion by TRAM-34 (10 μM) treatment in vitro in Con-A–differentiated peripheral T_{reg} cells. (A and C) Real-time PCR examinations for the transcriptional expression of IL-10 (A) and IL-17A (C) in vehicle- and TRAM-34–treated T_{reg} cells (n = 4 for each). Expression levels were expressed as a ratio to ACTB. (B and D) Quantitative detection of IL-10 (B) and IL-17A (D) by an ELISA assay in vehicle- and TRAM-34–treated $CD4^+CD25^+$ T_{reg} cells (n = 4 for each). Results are expressed as means ± S.E.M. $^{**}P < 0.01$ vs. the vehicle control (0 μM TRAM-34).

was upregulated by 10 μM TRAM-34 in T_{reg} cells induced in vitro (Fig. 7). These results strongly suggested that the inhibition of $K_{Ca}3.1$ in peripheral T_{reg} cells induced in vitro is a beneficial strategy for achieving efficient T_{reg} therapy for IBD.

Effects of TRAM-34 Treatment on the Phosphorylation of ERK1/2, AKT, STAT3, and SMAD2/3 and Effects of Their Inhibitors on IL-10 and IL-17A Secretion in Con-A–Differentiated T_{reg} Cells. The MAPK-ERK, TGF (transforming growth factor)-β1-SMAD2/3, JAK-STAT3, CN-NFAT, and PI3K/AKT/mTOR (mammalian target of rapamycin) signaling pathways are involved in the transcription of IL-10 and IL-17A (Martin et al., 2003; Bouhamdan et al., 2015). The blockade of $K_{Ca}3.1$ decreased Ca^{2+} influx through Ca^{2+} release–activated Ca^{2+} channels in activated lymphocytes, resulting in the suppression of their signaling pathways (Feske et al., 2015). Western blot analyses showed no significant changes in the protein expression levels of phosphorylated P-ERK1/2, P-AKT, P-STAT3, P-SMAD2, and P-SMAD3 after the treatment of 24 hours with 10 μM TRAM-34 in Con-A–differentiated $CD4^+CD25^+$ T_{reg} cells (n = 4 for each) (Fig. 8). In addition, the secretion of IL-10 and IL-17A in Con-A–differentiated $CD4^+CD25^+$ T_{reg} cells was not affected by treatment with the following inhibitors for 24 hours (n = 4 for each): an ERK1/2 inhibitor (1 μM SCH772984), AKT inhibitor (5 μM AZD5363), STAT3 inhibitor (10 μM 5,15- diphenylporphyrin), CN inhibitor (1 μM ciclosporin A), CaMKII inhibitor (1 μM KN62), and TGF-β receptor inhibitor (10 μM LY364947) in the absence (Supplemental Fig. 8, A and B) and presence (Supplemental Fig. 8, C and D) of 10 μM TRAM-34. These results suggested that these signaling pathways were not involved in the underlying mechanism of the $K_{Ca}3.1$ inhibition–induced promotion of IL-10 and IL-17A expression/production.

Discussion

The production of IL-10 is impaired by human T-cell subsets in patients with IBD, and the therapeutic potential of IL-10 is currently being evaluated in clinical trials for the treatment of IBD (Roncarolo et al., 2018). Recent studies have focused on the development of T_{reg} therapy for IBD (Soukou et al., 2018; Clough et al., 2020). $K_{Ca}3.1$ is a pivotal regulator of cytokine expression; however, its contribution to IL-10 production in T_{reg} cells has not yet been elucidated. The main results of the present study are as follows: 1) the disease activity of IBD was suppressed by the in vivo administration of a $K_{Ca}3.1$ inhibitor (1 mg/kg, s.c.) to IBD model mice (Figs. 1 and 2); 2) the in vivo administration of the $K_{Ca}3.1$ inhibitor induced an increase in IL-10 expression in T_{reg} cells in the recovery phase in IBD model mice (Fig. 3), with the upregulation of positive IL-10 TRs E4BP4, KLF4, and Blimp1 in the T_{reg} cells of IBD model mice (Fig. 4); and 3) IL-10 production was increased by an in vitro treatment with the $K_{Ca}3.1$ inhibitor in peripherally induced T_{reg} cells, which was consistent with the upregulation of IL-10 TRs (Figs. 6 and 7). The upregulation of $K_{Ca}3.1$ in proinflammatory $CD4^+CD25^-$ T cells in acute IBD model mice was recovered, together with the attenuation of the pathogenesis of IBD (Ohya et al., 2014), and $K_{Ca}3.1$ was post-translationally

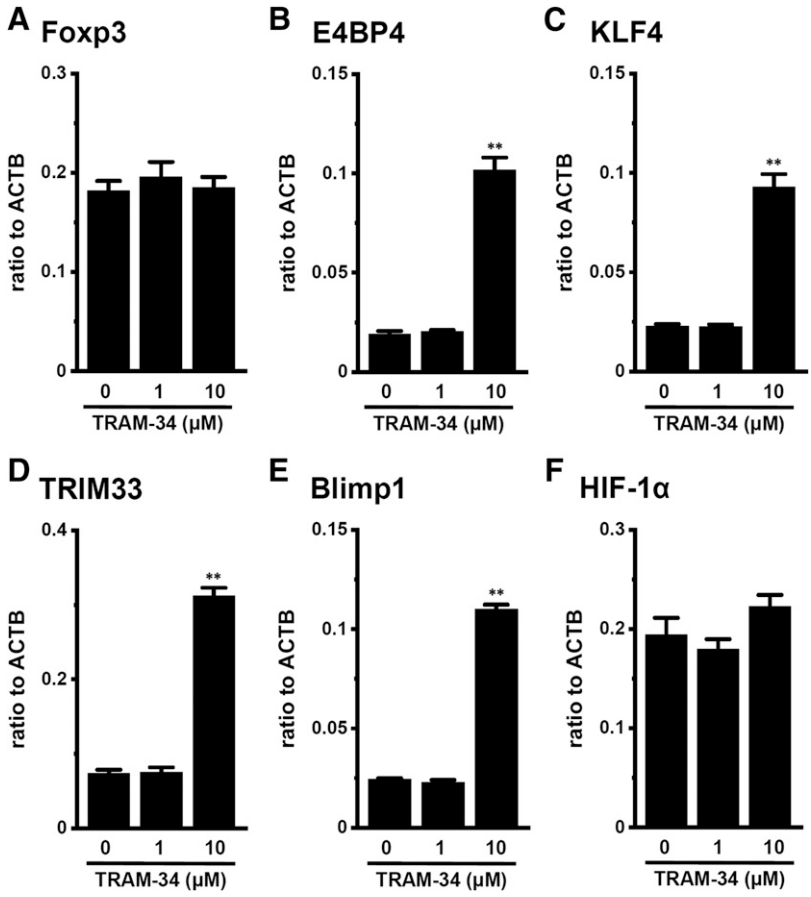

Fig. 7. Changes in expression levels of transcriptional regulators of IL-10 and/or IL-17A by TRAM-34 treatment in vitro in Con-A–differentiated peripheral T_{reg} cells. (A–F) Real-time PCR examinations for the transcriptional expression of Foxp3 (A), E4BP4 (B), KLF4 (C), TRIM33 (D), Blimp1 (E), and HIF-1α (F) in vehicle- and TRAM-34–treated $CD4^+CD25^+$ T_{reg} cells (n = 4 for each). Expression levels were expressed as a ratio to ACTB. Results are expressed as means ± S.E.M. $^{**}P < 0.01$ vs. the vehicle control (0 μM TRAM-34).

regulated by the histone deacetylases HDAC2 and HDAC3 in these cells (Matsui et al., 2018). The upregulation of $K_{Ca}3.1$, HDAC2, and HDAC3 in the mLN T_{reg} cells of IBD model mice in the recovery phase was not detected in the present study (Supplemental Fig. 5, A–C). Since the population of $CD4^+CD25^+$ subsets was almost 10%–15% of the $CD4^+$ subset (less than 3% of all mLN cells) (Supplemental Figure 4), difficulties were associated with examining the in vitro effects of the $K_{Ca}3.1$ inhibitor on IL-10 secretion using the isolated T_{reg} cells of IBD model mice. Accordingly, to elucidate the transcriptional mechanism enhancing IL-10 expression and secretion by the inhibition of $K_{Ca}3.1$, $CD4^+CD25^+$ T_{reg} cells peripherally induced in vitro by a lectin stimulation were used.

Recent studies reported that IL-17A plays a protective role against IBD (Bellemore et al., 2015; Gagliani et al., 2015), and in DSS-induced IBD model mice, protective IL-17A reflects the chronic stage of disease (O'Connor et al., 2009). A large population of IL-17A–producing $CD4^+CD25^+Foxp3^+$ T_{reg} (also referred to as Th17-like T_{reg}) cells has been reported in patients with IBD and an IBD mouse model (Li and Boussiotis, 2013; Hovhannisyan et al., 2011; Kryczek et al., 2011). Th17-like T_{reg} cells have also been found in patients with rheumatoid arthritis, multiple sclerosis, and severe psoriasis (Kryczek et al., 2011; Pandiyan and Zhu, 2015). The present study showed that IL-17A was also upregulated by the inhibition of $K_{Ca}3.1$ in the T_{reg} cells of IBD model mice and Con-A–differentiated T_{reg} cells (Figs. 5 and 7). During the resolution of inflammation, Th17 cells transdifferentiate into T_{reg} cells (Bellemore et al., 2015). Therefore, the inhibition of $K_{Ca}3.1$ may be crucial for differentiation into IL-17A–expressing T_{reg} cells, which play a protective role in the recovery phase of IBD.

A number of the TRs of IL-10 and IL-17A have been identified in lymphoid and myeloid cells, including T_{reg} cells (Jung et al., 2017; Capone and Volpe, 2020; Fang and Zhu, 2020). As shown in Figs. 4 and 7, the TRs promoting IL-10 and/or IL-17A expression in various T-cell subsets—namely, E4BP4, KLF4, and Blimp1—are commonly upregulated by TRAM-34 in T_{reg} cells in the recovery phase in IBD model mice and Con-A–differentiated T_{reg} cells. KLF4 has been identified as a positive TR for IL-10 and IL-17A in macrophages and Th17 cells (Liu et al., 2007; An et al., 2011), and KLF4 was found to be upregulated in goblet cells from patients with Crohn disease (Gersemann et al., 2009). Fujimoto et al. (2019) recently showed that the ablation of KLF4 resulted in the hyperphosphorylation of SMAD2 and elevated nuclear localization of P-SMAD2/3. Smad2 regulates $CD4^+$ T-cell differentiation into induced T_{reg} cells and Th17 cells (Malhotra et al., 2010). However, discrepancies exist in the findings reported—namely, $K_{Ca}3.1$ blockers and activators both attenuated Smad2/3 phosphorylation (Yu et al., 2014; Roach et al., 2015; Matsui et al., 2019). One hypothesis to explain the $K_{Ca}3.1$ inhibitor–induced increase in IL-10 expression is that the inhibition of $K_{Ca}3.1$ enhances KLF4-mediated SMAD2 phosphorylation in T_{reg} cells. However, the inhibition of $K_{Ca}3.1$ did not affect the phosphorylation of SMAD2/3 (Fig. 8, F and G). We previously reported that the nuclear localization of P-SMAD2 was regulated by $K_{Ca}3.1$; however, in the present study, no significant changes in the nuclear localization of P-SMAD2/3 were found after TRAM-34 treatment in Con-A–differentiated

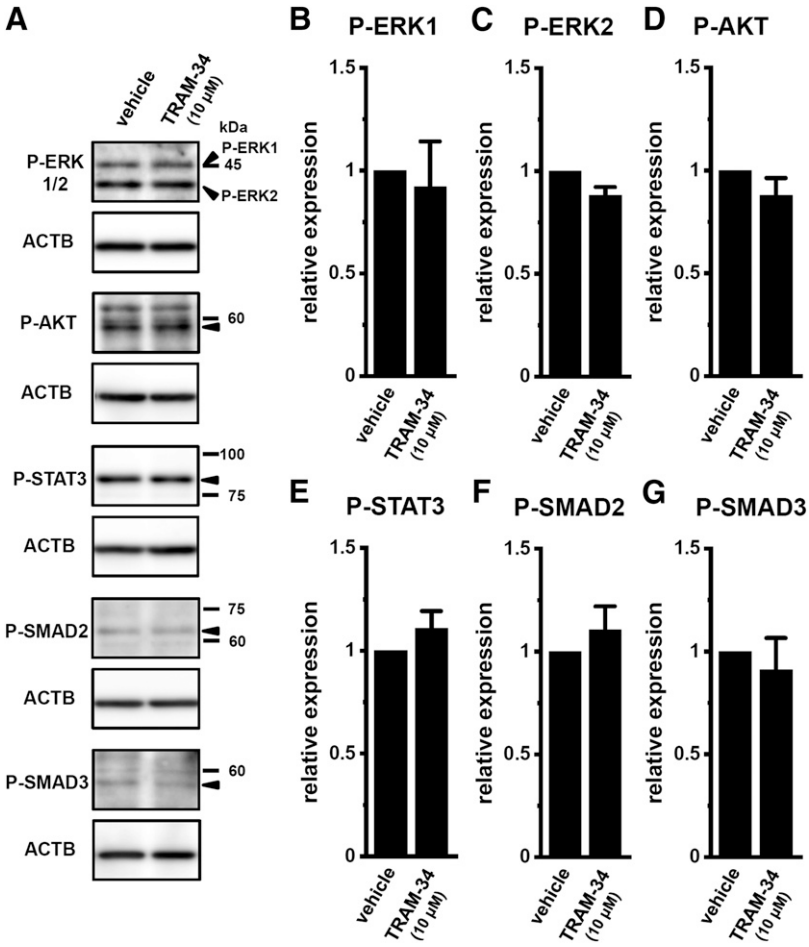

Fig. 8. No changes in protein expression levels of phosphorylated P-ERK1/2, P-AKT, P-STAT3, P-SMAD2, or P-SMAD3 after TRAM-34 treatment in vitro in Con-A–differentiated peripheral T_{reg} cells. (A) Western blot showing P-ERK1/2, P-AKT, P-STAT3, P-SMAD2, and P-SMAD3 in vehicle- and TRAM-34–treated $CD4^+CD25^+$ T_{reg} cells. (B–G) Summarized results of the relative protein expression of P-ERK1/2, P-AKT, P-STAT3, P-SMAD2, and P-SMAD3 were obtained by measuring the optical density of band signals at approximately 45/40 (P-ERK1/2), 60 (P-AKT), 85 (P-STAT3), 60 (P-SMAD2), and 55 (P-SMAD3) kDa. After compensation with the optical density of the ACTB signal (43 kDa), the expression level in the vehicle control was expressed as 1.0 (n = 4 for each). Results were expressed as means ± S.E.M.

T_{reg} cells (Supplemental Fig. 9). The MAPK-ERK, PI3K-AKT, and CN-NFAT signaling pathways are generally regulated in a Ca^{2+}-dependent manner. Therefore, intracellular Ca^{2+} influx by the inhibition of $K_{Ca}3.1$ attenuates these signaling pathways. A previous study reported that $K_{Ca}3.1$ inhibition–induced increases in intracellular K^+ concentrations may be attenuated by the AKT signaling pathway (Eil et al., 2016). KLF4 expression may be positively and negatively regulated by the AKT and ERK signaling pathways (Riverso et al., 2017; Liu et al., 2017; Dong et al., 2019). However, the inhibition of $K_{Ca}3.1$ did not affect the phosphorylation of ERK1/2 or AKT (Fig. 8), and their inhibitors did not alter the secretion of IL-10 or IL-17A (Supplemental Fig. 8). Although KLF4 is also activated by the JAK-STAT3 signaling pathway, the inhibition of $K_{Ca}3.1$ did not affect the phosphorylation of STAT3 (Fig. 8), and a STAT3 inhibitor did not alter the secretion of IL-10 or IL-17A (Supplemental Fig. 8). Further studies are needed to elucidate the mechanisms underlying the $K_{Ca}3.1$ inhibition–induced upregulation of KLF4 in IL-17A–expressing T_{reg} cells in the recovery phase in IBD model mice.

The transcription of E4BP4 is activated through the MAPK-ERK, PI3K-AKT, CN-NFAT, TGF-β-SMAD, and CaMK signaling pathways (Nishimura and Tanaka, 2001; Motomura et al., 2011; Kim et al., 2019). The attenuation of intracellular Ca^{2+} influx by the inhibition of $K_{Ca}3.1$ was shown to prevent the Ca^{2+}-dependent CaMK signaling pathway in addition to the ERK, AKT, and CN-NFAT signaling pathways. In contrast, Simma et al. (2014) reported that its inhibition activated the ERK, AKT, and CN-NFAT signaling pathways, resulting in an increase in IL-10 expression in activated B cells. The present study revealed no significant changes in IL-10 and IL-17A secretion (Supplemental Fig. 8) after the pharmacological blockade of the ERK, CN-NFAT, and CaMK signaling pathways in the absence and presence of TRAM-34, thereby strongly supporting the lack of involvement of these signaling pathways in the $K_{Ca}3.1$ inhibition–induced upregulation of E4BP4. Moreover, Blimp1 was shown to increase IL-10 expression in various T-cell subsets, and its expression was modulated by the MAPK-ERK, PI3K-AKT, and TGF-β-SMAD signaling pathways (Sciortino et al., 2017; Setz et al., 2018). Blimp1 was not upregulated in T_{reg} cells in the recovery phase in IBD model mice (Fig. 4). In this study, we did not examine the effects of TRAM-34 on the activities of TR candidates possibly involved in IL-10 and/or IL-17A expression in T_{reg} cells. Further studies will be needed to determine which TRs are major contributors of IL-10/IL-17A transcription. It is also important to clarify the mechanisms underlying the $K_{Ca}3.1$ inhibition–induced upregulation of TRs in T_{reg} cells in the recovery phase in IBD model mice.

Hypoxia is involved in intestinal inflammation in patients with IBD, and the activation of HIF-1α promotes T_{reg} cell activity, such as IL-10 expression, without altering Foxp3 expression (Colgan and Taylor, 2010; Sakaki-Yumoto et al., 2013; Westendorf et al., 2017). As shown in Fig. 4D, the expression level of HIF-1α was high, possibly as a result of enhanced oxygen consumption in the diseased area. On the

other hand, improvement of IBD symptoms by the administration of TRAM-34 suppressed the expression level of HIF-1α (Fig. 4H), possibly as a result of escape from hypoxic condition. HIF-1α enhances IL-10 expression by directly binding the promoter and also enhances IL-17A through the RORγt-mediated activation of the promoter (Flück and Fandrey, 2016; Westendorf et al., 2017). However, HIF-1α expression was negatively regulated by the in vivo administration of the $K_{Ca}3.1$ inhibitor (Fig. 4H), suggesting that HIF-1α did not contribute to the $K_{Ca}3.1$ inhibition–induced upregulation of IL-10 and IL-17A.

In conclusion, the present results strongly suggest the potential of $K_{Ca}3.1$ in peripherally induced T_{reg} cells as a target for more efficient T_{reg} therapy for chronic inflammatory disorders and also suggest that treatments with $K_{Ca}3.1$ inhibitor in T_{reg} cells may effectively increase IL-10 production. Protective effects during the disease process of IBD may involve peripherally induced IL-10–producing T_{reg} cells (Mayne and Williams, 2013; Meng et al., 2018), and recombinant IL-10 therapy was previously shown to ameliorate established T-cell transfer colitis (Mizoguchi et al., 2020). Recent clinical studies focused on the development of T_{reg} cell therapy for Crohn disease to provide a continuous source of anti-inflammatory cytokines, such as IL-10, and thus achieve a meaningful therapeutic outcome. The manipulation of IL-10^{high} T_{reg} cells by the inhibition/knockdown of $K_{Ca}3.1$ may be beneficial in the treatment of chronic inflammatory diseases.

Acknowledgments

We thank Hiroki Niguma and Rina Shibaoka for their technical assistance. Medical English Service (Kyoto, Japan) reviewed the manuscript prior to submission.

Authorship Contributions

Participated in research design: Ohya, Matsui.

Conducted experiments: Ohya, Matsui, Kajikuri, Endo, Kito.

Performed data analysis: Ohya, Matsui, Kajikuri, Endo, Kito.

Wrote or contributed to the writing of the manuscript: Ohya, Matsui, Kajikuri, Endo, Kito.

References

An J, Golech S, Klaewsongkram J, Zhang Y, Subedi K, Huston GE, Wood WH 3rd, Wersto RP, Becker KG, Swain SL, et al. (2011) Krüppel-like factor 4 (KLF4) directly regulates proliferation in thymocyte development and IL-17 expression during Th17 differentiation. *FASEB J* **25**:3634–3645.

Bellemore SM, Nikoopour E, Schwartz JA, Krougly O, Lee-Chan E, and Singh B (2015) Preventative role of interleukin-17 producing regulatory T helper type 17 (Treg 17) cells in type 1 diabetes in non-obese diabetic mice. *Clin Exp Immunol* **182**:261–269.

Bento AF, Leite DF, Marcon R, Claudino RF, Dutra RC, Cola M, Martini AC, and Calixto JB (2012) Evaluation of chemical mediators and cellular response during acute and chronic gut inflammatory response induced by dextran sodium sulfate in mice. *Biochem Pharmacol* **84**:1459–1469.

Bouhamdan M, Bauerfeld C, Talreja J, Beuret L, Charron J, and Samavati L (2015) MEK1 dependent and independent ERK activation regulates IL-10 and IL-12 production in bone marrow derived macrophages. *Cell Signal* **27**:2068–2076.

Capone A and Volpe E (2020) Transcriptional regulators of T helper 17 cell differentiation in health and autoimmune diseases. *Front Immunol* **11**:348.

Chassaing B, Aitken JD, Malleshappa M, and Vijay-Kumar M (2014) Dextran sulfate sodium (DSS)-induced colitis in mice. *Curr Protoc Immunol* **104**:15.25.1–15.25.14.

Clough JN, Omer OS, Tasker S, Lord GM, and Irving PM (2020) Regulatory T-cell therapy in Crohn's disease: challenges and advances. *Gut* **69**:942–952.

Colgan SP and Taylor CT (2010) Hypoxia: an alarm signal during intestinal inflammation. *Nat Rev Gastroenterol Hepatol* **7**:281–287.

Di L, Srivastava S, Zhdanova O, Ding Y, Li Z, Wulff H, Lafaille M, and Skolnik EY (2010) Inhibition of the K^+ channel KCa3.1 ameliorates T cell-mediated colitis. *Proc Natl Acad Sci USA* **107**:1541–1546.

Dieleman LA, Palmen MJ, Akol H, Bloemena E, Peña AS, Meuwissen SG, and Van Rees EP (1998) Chronic experimental colitis induced by dextran sulphate sodium (DSS) is characterized by Th1 and Th2 cytokines. *Clin Exp Immunol* **114**:385–391.

Dong X, Wang F, Xue Y, Lin Z, Song W, Yang N, and Li Q (2019) MicroRNA-9-5p downregulates Klf4 and influences the progression of hepatocellular carcinoma via the AKT signaling pathway. *Int J Mol Med* **43**:1417–1429.

Eichele DD and Kharbanda KK (2017) Dextran sodium sulfate colitis murine model: an indispensable tool for advancing our understanding of inflammatory bowel diseases pathogenesis. *World J Gastroenterol* **23**:6016–6029.

Eil R, Vodnala SK, Clever D, Klebanoff CA, Sukumar M, Pan JH, Palmer DC, Gros A, Yamamoto TN, Patel SJ, et al. (2016) Ionic immune suppression within the tumour microenvironment limits T cell effector function. *Nature* **537**:539–543.

Fakhoury M, Negrulj R, Mooranian A, and Al-Salami H (2014) Inflammatory bowel disease: clinical aspects and treatments. *J Inflamm Res* **7**:113–120.

Fang D and Zhu J (2020) Molecular switches for regulating the differentiation of inflammatory and IL-10-producing anti-inflammatory T-helper cells. *Cell Mol Life Sci* **77**:289–303.

Feske S, Wulff H, and Skolnik EY (2015) Ion channels in innate and adaptive immunity. *Annu Rev Immunol* **33**:291–353.

Flück K and Fandrey J (2016) Oxygen sensing in intestinal mucosal inflammation. *Pflugers Arch* **468**:77–84.

Fujimoto S, Hayashi R, Hara S, Sasamoto Y, Harrington J, Tsujikawa M, and Nishida K (2019) KLF4 prevents epithelial to mesenchymal transition in human corneal epithelial cells *via* endogenous TGF-β2 suppression. *Regen Ther* **11**: 249–257.

Gagliani N, Amezcua Vesely MC, Iseppon A, Brockmann L, Xu H, Palm NW, de Zoete MR, Licona-Limón P, Paiva RS, Ching T, et al. (2015) T_h17 cells transdifferentiate into regulatory T cells during resolution of inflammation. *Nature* **523**:221–225.

Gersemann M, Becker S, Kübler I, Koslowski M, Wang G, Herrlinger KR, Griger J, Fritz P, Fellermann K, Schwab M, et al. (2009) Differences in goblet cell differentiation between Crohn's disease and ulcerative colitis. *Differentiation* **77**:84–94.

Hovhannisyan Z, Treatman J, Littman DR, and Mayer L (2011) Characterization of interleukin-17-producing regulatory T cells in inflamed intestinal mucosa from patients with inflammatory bowel diseases. *Gastroenterology* **140**:957–965.

Jung MK, Kwak JE, and Shin EC (2017) IL-17A-producing $Foxp3^+$ regulatory T cells and human diseases. *Immune Netw* **17**:276–286.

Kaplan GG (2015) The global burden of IBD: from 2015 to 2025. *Nat Rev Gastroenterol Hepatol* **12**:720–727.

Kennedy RJ, Hoper M, Deodhar K, Erwin PJ, Kirk SJ, and Gardiner KR (2000) Interleukin 10-deficient colitis: new similarities to human inflammatory bowel disease. *Br J Surg* **87**:1346–1351.

Kim HS, Sohn H, Jang SW, and Lee GR (2019) The transcription factor NFIL3 controls regulatory T-cell function and stability. *Exp Mol Med* **51**:80.

Kryczek I, Wu K, Zhao E, Wei S, Vatan L, Szeliga W, Huang E, Greenson J, Chang A, Roliński J, et al. (2011) IL-17^+ regulatory T cells in the microenvironments of chronic inflammation and cancer. *J Immunol* **186**:4388–4395.

Li L and Boussiotis VA (2013) The role of IL-17-producing $Foxp3^+$ $CD4^+$ T cells in inflammatory bowel disease and colon cancer. *Clin Immunol* **148**:246–253.

Liu CH, Huang Q, Jin ZY, Zhu CL, Liu Z, and Wang C (2017) miR-21 and KLF4 jointly augment epithelial-mesenchymal transition via the Akt/ERK1/2 pathway. *Int J Oncol* **50**:1109–1115.

Liu J, Zhang H, Liu Y, Wang K, Feng Y, Liu M, and Xiao X (2007) KLF4 regulates the expression of interleukin-10 in RAW264.7 macrophages. *Biochem Biophys Res Commun* **362**:575–581.

Malhotra N, Robertson E, and Kang J (2010) SMAD2 is essential for TGF β-mediated Th17 cell generation. *J Biol Chem* **285**:29044–29048.

Martin M, Schifferle RE, Cuesta N, Vogel SN, Katz J, and Michalek SM (2003) Role of the phosphatidylinositol 3 kinase-Akt pathway in the regulation of IL-10 and IL-12 by Porphyromonas gingivalis lipopolysaccharide. *J Immunol* **171**:717–725.

Matsui M, Kajikuri J, Kito H, Endo K, Hasegawa Y, Murate S, and Ohya S (2019) Inhibition of interleukin 10 transcription through SMAD2/3 signaling pathway by Ca^{2+}-activated K^+ channel $K_{Ca}3.1$ activation in human lymphoma HuT-78 cells. *Mol Pharmacol* **95**:294–302.

Matsui M, Terasawa K, Kajikuri J, Kito H, Endo K, Jaikhan P, Suzuki T, and Ohya S (2018) Histone deacetylases enhance Ca^{2+}-activated K^+ channel $K_{Ca}3.1$ expression in murine inflammatory $CD4^+$ T cells. *Int J Mol Sci* **19**:2942.

Mayne CG and Williams CB (2013) Induced and natural regulatory T cells in the development of inflammatory bowel disease. *Inflamm Bowel Dis* **19**:1772–1788.

Meng X, Grötsch B, Luo Y, Knaup KX, Wiesener MS, Chen XX, Jantsch J, Fillatreau S, Schett G, and Bozec A (2018) Hypoxia-inducible factor-1α is a critical transcription factor for IL-10-producing B cells in autoimmune disease. *Nat Commun* **9**: 251.

Mizoguchi E, Low D, Ezaki Y, and Okada T (2020) Recent updates on the basic mechanisms and pathogenesis of inflammatory bowel diseases in experimental animal models. *Intest Res* **18**:151–167.

Motomura Y, Kitamura H, Hijikata A, Matsunaga Y, Matsumoto K, Inoue H, Atarashi K, Hori S, Watarai H, Zhu J, et al. (2011) The transcription factor E4BP4 regulates the production of IL-10 and IL-13 in CD4+ T cells. *Nat Immunol* **12**: 450–459.

Nakakura S, Matsui M, Sato A, Ishii M, Endo K, Muragishi S, Murase M, Kito H, Niguma H, Kurokawa N, et al. (2015) Pathophysiological significance of the two-pore domain $K^{(+)}$ channel $K_{2P}5.1$ in splenic CD4(+)CD25(-) T cell subset from a chemically-induced murine inflammatory bowel disease model. *Front Physiol* **6**: 299.

Neumann C, Scheffold A, and Rutz S (2019) Functions and regulation of T cell-derived interleukin-10. *Semin Immunol* **44**:101344.

Ng TH, Britton GJ, Hill EV, Verhagen J, Burton BR, and Wraith DC (2013) Regulation of adaptive immunity; the role of interleukin-10. *Front Immunol* **4**:129.

Nishimura Y and Tanaka T (2001) Calcium-dependent activation of nuclear factor regulated by interleukin 3/adenovirus E4 promoter-binding protein gene expression by calcineurin/nuclear factor of activated T cells and calcium/calmodulin-dependent protein kinase signaling. *J Biol Chem* **276**:19921–19928.

Ohya S, Fukuyo Y, Kito H, Shibaoka R, Matsui M, Niguma H, Maeda Y, Yamamura H, Fujii M, Kimura K, et al. (2014) Upregulation of KCa3.1 K(+) channel in mesenteric lymph node CD4(+) T lymphocytes from a mouse model of dextran sodium sulfate-induced inflammatory bowel disease. *Am J Physiol Gastrointest Liver Physiol* **306**:G873–G885.

O'Connor W Jr, Kamanaka M, Booth CJ, Town T, Nakae S, Iwakura Y, Kolls JK, and Flavell RA (2009) A protective function for interleukin 17A in T cell-mediated intestinal inflammation. *Nat Immunol* **10**:603–609.
Pandiyan P and Zhu J (2015) Origin and functions of pro-inflammatory cytokine producing Foxp3$^+$ regulatory T cells. *Cytokine* **76**:13–24.
Riverso M, Montagnani V, and Stecca B (2017) KLF4 is regulated by RAS/RAF/MEK/ERK signaling through E2F1 and promotes melanoma cell growth. *Oncogene* **36**: 3322–3333.
Roach KM, Feghali-Bostwick C, Wulff H, Amrani Y, and Bradding P (2015) Human lung myofibroblast TGFβ1-dependent Smad2/3 signalling is Ca(2+)-dependent and regulated by KCa3.1 K(+) channels. *Fibrogenesis Tissue Repair* **8**:5.
Roncarolo MG, Gregori S, Bacchetta R, Battaglia M, and Gagliani N (2018) The biology of T regulatory type 1 cells and their therapeutic application. *Immunity* **49**: 1004–1019.
Rutz S and Ouyang W (2016) Regulation of interleukin-10 expression. *Adv Exp Med Biol* **941**:89–116.
Sakaki-Yumoto M, Liu J, Ramalho-Santos M, Yoshida N, and Derynck R (2013) Smad2 is essential for maintenance of the human and mouse primed pluripotent stem cell state. *J Biol Chem* **288**:18546–18560.
Sciortino M, Camacho-Leal MDP, Orso F, Grassi E, Costamagna A, Provero P, Tam W, Turco E, Defilippi P, Taverna D, et al. (2017) Dysregulation of Blimp1 transcriptional repressor unleashes p130Cas/ErbB2 breast cancer invasion. *Sci Rep* **7**: 1145.
Setz CS, Hug E, Khadour A, Abdelrasoul H, Bilal M, Hobeika E, and Jumaa H (2018) PI3K-mediated Blimp-1 activation controls B cell selection and homeostasis. *Cell Rep* **24**:391–405.
Sha T, Igaki K, Yamasaki M, Watanabe T, and Tsuchimori N (2013) Establishment and validation of a new semi-chronic dextran sulfate sodium-induced model of colitis in mice. *Int Immunopharmacol* **15**:23–29.
Shah N, Kammermeier J, Elawad M, and Glocker EO (2012) Interleukin-10 and interleukin-10-receptor defects in inflammatory bowel disease. *Curr Allergy Asthma Rep* **12**:373–379.
Shanmugasundaram R and Selvaraj RK (2011) Regulatory T cell properties of chicken CD4$^+$CD25$^+$ cells. *J Immunol* **186**:1997–2002.
Simma N, Bose T, Kahlfuss S, Mankiewicz J, Lowinus T, Lühder F, Schüler T, Schraven B, Heine M, and Bommhardt U (2014) NMDA-receptor antagonists block B-cell function but foster IL-10 production in BCR/CD40-activated B cells. *Cell Commun Signal* **12**:75.
Singh P, Ananthakrishnan A, and Ahuja V (2017) Pivot to Asia: inflammatory bowel disease burden. *Intest Res* **15**:138–141.
Soukou S, Brockmann L, Bedke T, Gagliani N, Flavell RA, and Huber S (2018) Role of IL-10 receptor signaling in the function of CD4$^+$ T-regulatory type 1 cells: T-cell therapy in patients with inflammatory bowel disease. *Crit Rev Immunol* **38**: 415–431.
Süss C, Broncy L, Pollinger K, Kunst C, Gülow K, Müller M, and Wölfel G (2020) *KCNN4* expression is elevated in inflammatory bowel disease: this might be a novel marker and therapeutic option targeting potassium channels. *J Gastrointestin Liver Dis* **29**:539–547.
Tagishi K, Shimizu A, Endo K, Kito H, Niwa S, Fujii M, and Ohya S (2016) Defective splicing of the background K$^+$ channel $K_{2P}5.1$ by the pre-mRNA splicing inhibitor, pladienolide B in lectin-activated mouse splenic CD4$^+$ T cells. *J Pharmacol Sci* **132**: 205–209.
Tanaka S, Jiang Y, Martinez GJ, Tanaka K, Yan X, Kurosaki T, Kaartinen V, Feng XH, Tian Q, Wang X, et al. (2018) Trim33 mediates the proinflammatory function of Th17 cells. *J Exp Med* **215**:1853–1868.
Westendorf AM, Skibbe K, Adamczyk A, Buer J, Geffers R, Hansen W, Pastille E, and Jendrossek V (2017) Hypoxia enhances immunosuppression by inhibiting CD4$^+$ effector T cell function and promoting Treg activity. *Cell Physiol Biochem* **41**:1271–1284.
Yu Z, Yu P, Chen H, and Geller HM (2014) Targeted inhibition of KCa3.1 attenuates TGF-β-induced reactive astrogliosis through the Smad2/3 signaling pathway. *J Neurochem* **130**:41–49.

Address correspondence to: Susumu Ohya, Department of Pharmacology, Graduate School of Medical Sciences, Nagoya City University, 1 Kawasumi, Mizuho-cho, Mizuho-ku, Nagoya 467-8601, Aichi, Japan. E-mail: sohya@med.nagoya-cu.ac.jp

JPET-AR-2020-000395-R2

SUPPLEMENTARY DATA

Increased IL-10 expression by the inhibition of $K_{Ca}3.1$ in $CD4^+CD25^+$ regulatory T cells in the recovery phase in an inflammatory bowel disease mouse model

Susumu Ohya*, Miki Matsui*, Junko Kajikuri, Kyoko Endo, Hiroaki Kito

Department of Pharmacology, Graduate School of Medical Sciences, Nagoya City University, Nagoya 467-8601, Japan (S.O., M.M., J.K., K.E., H.K.)

*: These authors contributed equally to this work.

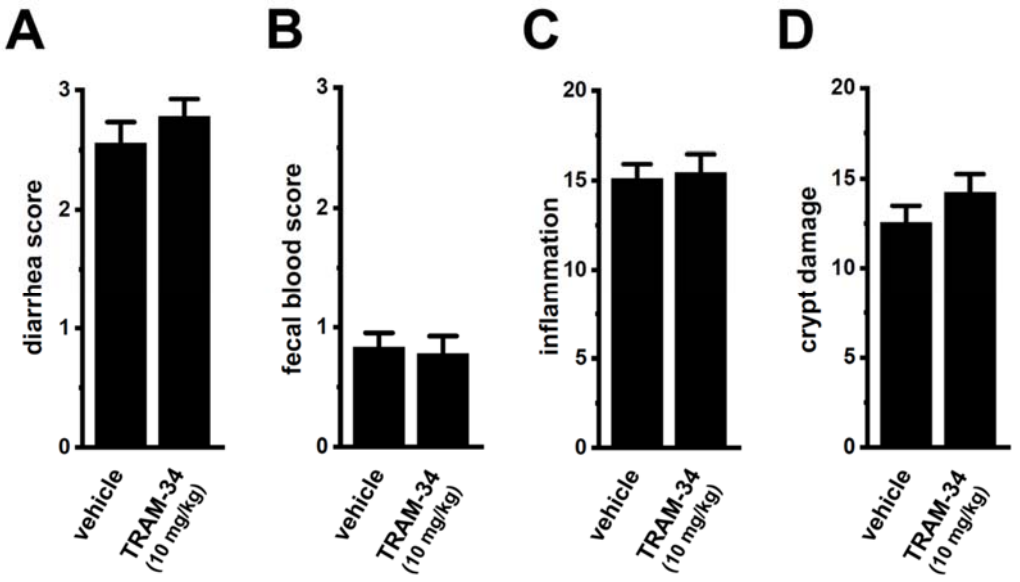

Figure S1. Effects of the s.c. administration of TRAM-34 (10 mg/kg, s.c.) on the clinical assessment (diarrhea and bloody feces) and colonic inflammation in IBD model mice. A, B: Therapeutic effects of repeated administration of TRAM-34 (10 mg/kg, s.c.) on diarrhea (A) and visible fecal blood (B) scores in recovery phase of IBD model mice. C, D: Colon damage (inflammation and crypt damage scores) was assessed histologically. Results were expressed as means ± SEM (n = 9 for each).

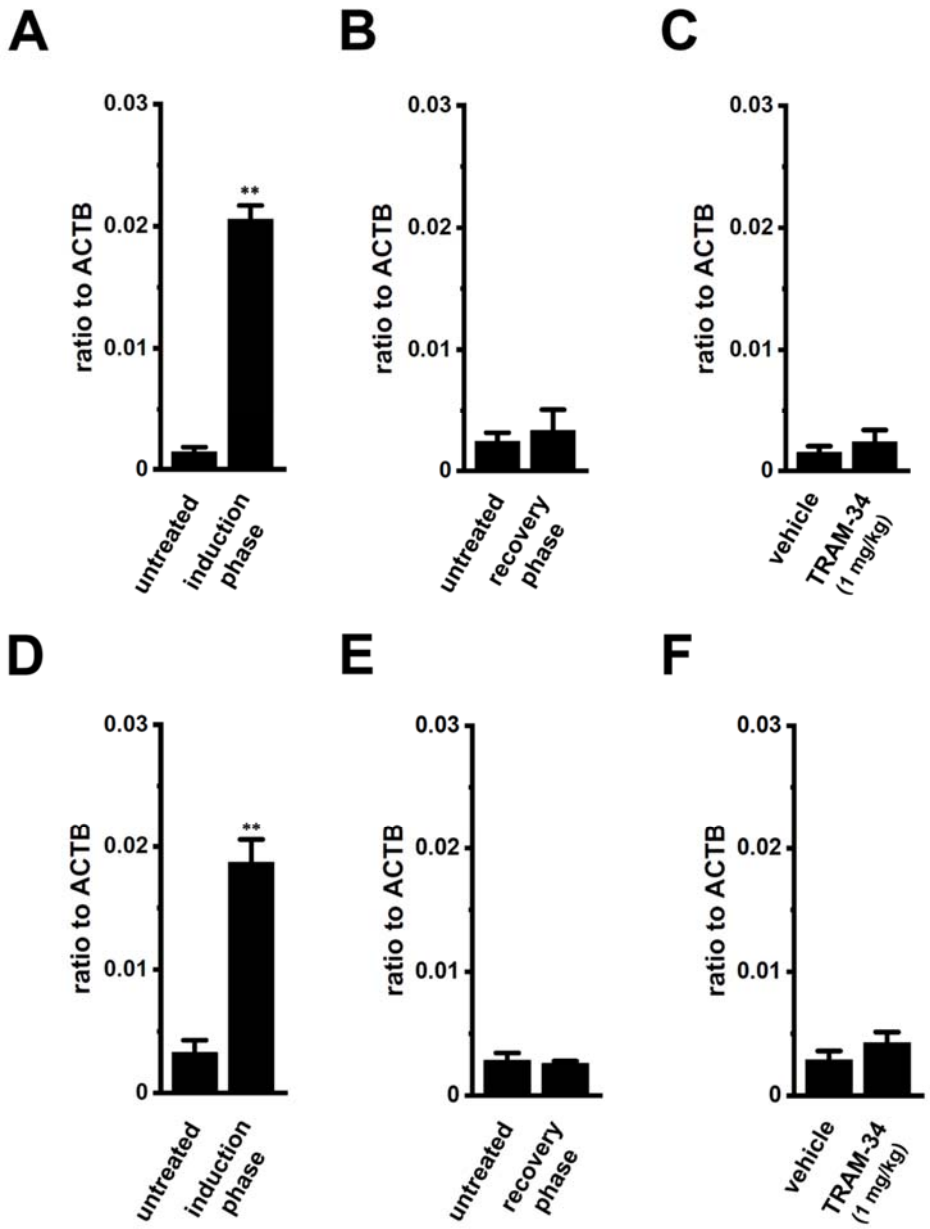

Figure S2. Expression levels of pro-inflammatory cytokines (IFN-γ and IL-17F) in mLN CD4$^+$CD25$^-$ T cells in the induction and recovery phases in IBD model mice. A-F: Real-time PCR examinations for the expression of IFN-γ (A-C) and IL-17F (D-F) transcripts in mLN T_{reg} cells in the untreated and induction phases on day 7 (A, D), in the untreated and recovery phases on day 12 (B, E), and in the recovery phases in IBD model mice *in vivo* administered vehicle and TRAM-34 (1 mg/kg) (C, F) (n = 4 for each). Expression levels were expressed as a ratio to ACTB. Results are expressed as means ± SEM. **: $P < 0.01$ vs. untreated mice on day 7.

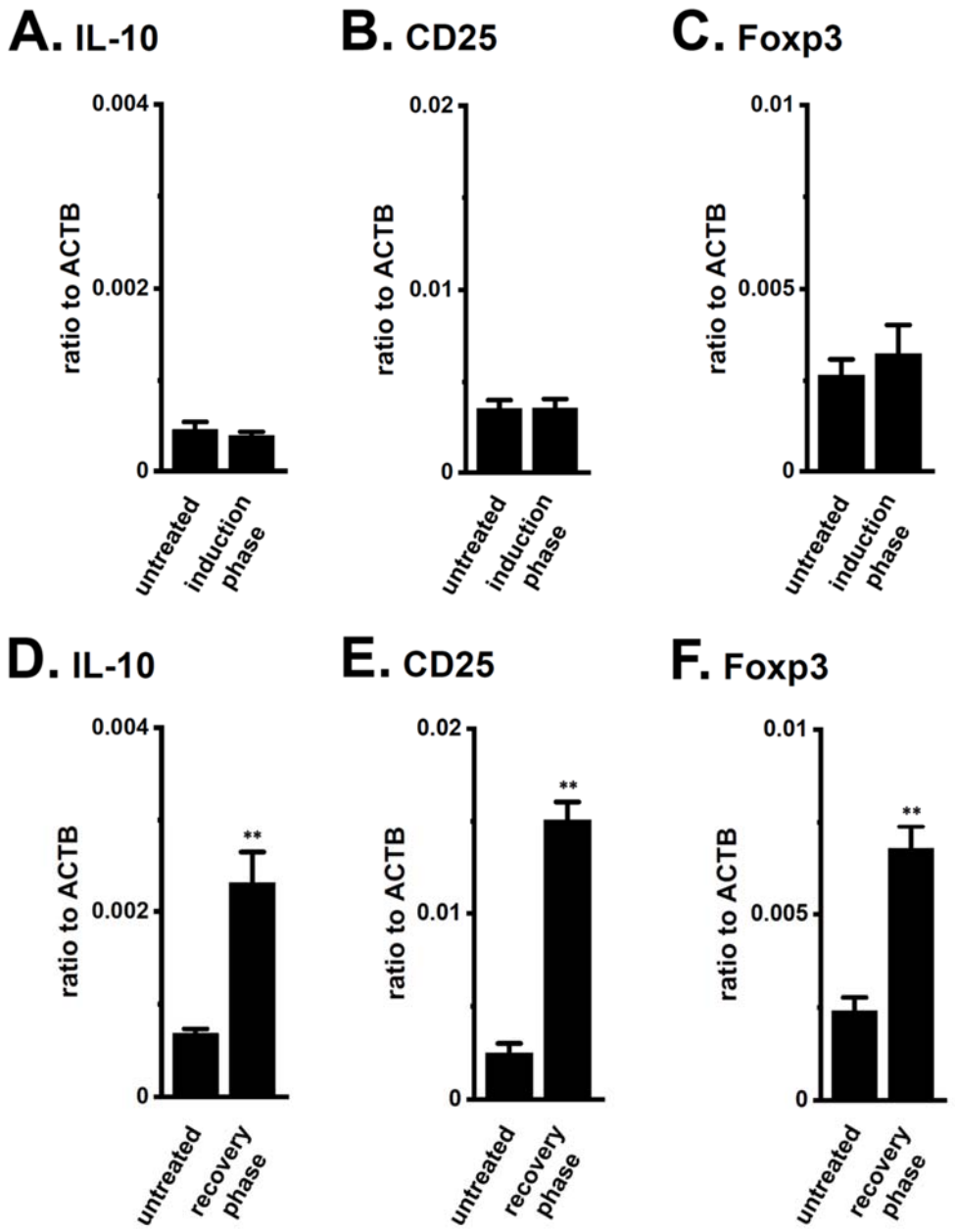

Figure S3. Increased IL-10, CD25, and Foxp3 expression in mLN tissues in the recovery phase in IBD model mice, but not in the induction phase. A-F: Real-time PCR examinations for the transcriptional expression of IL-10 (A, D), CD25 (B, E), and Foxp3 (C, F) in the mLN tissues of untreated mice (A-C on day 7 and D-F on day 12), IBD model mice in the induction phase (A-C), and IBD model mice in the recovery phase (D-F) (n = 4 for each). Expression levels were expressed as a ratio to ACTB. Results are expressed as means ± SEM. **: $P < 0.01$ vs. untreated mice.

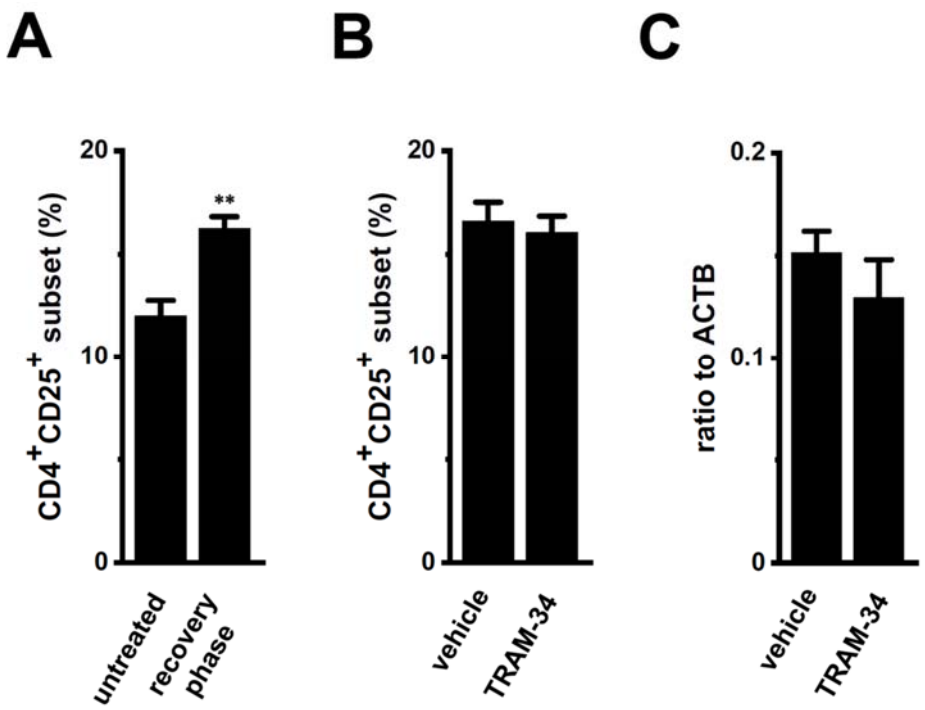

Figure S4. Effects of TRAM-34 (1 mg/kg, s.c.) administration on the population of the $CD4^+CD25^+$ T_{reg} cell subset and the expression level of CD25 in $CD4^+CD25^+$ T_{reg} cells. A, B: Comparison of the population of the $CD4^+CD25^+$ T_{reg} cell subset relative to $CD4^+$ T cells between untreated mice and IBD model mice in the recovery phase (n = 4 for each) (A) and between vehicle- and TRAM-34-treated IBD model mice (n = 5 for each) (B) by flow cytometry using antibodies labeled with different fluorophores (FITC-CD4 and PE-CD25). C: Real-time PCR examinations for the transcriptional expression of CD25 in vehicle- and TRAM-34-administered $CD4^+CD25^+$ T_{reg} cells (n = 5 for each). Expression levels were expressed as a ratio to ACTB. Results are expressed as means ± SEM. **: $P < 0.01$ vs. untreated mice.

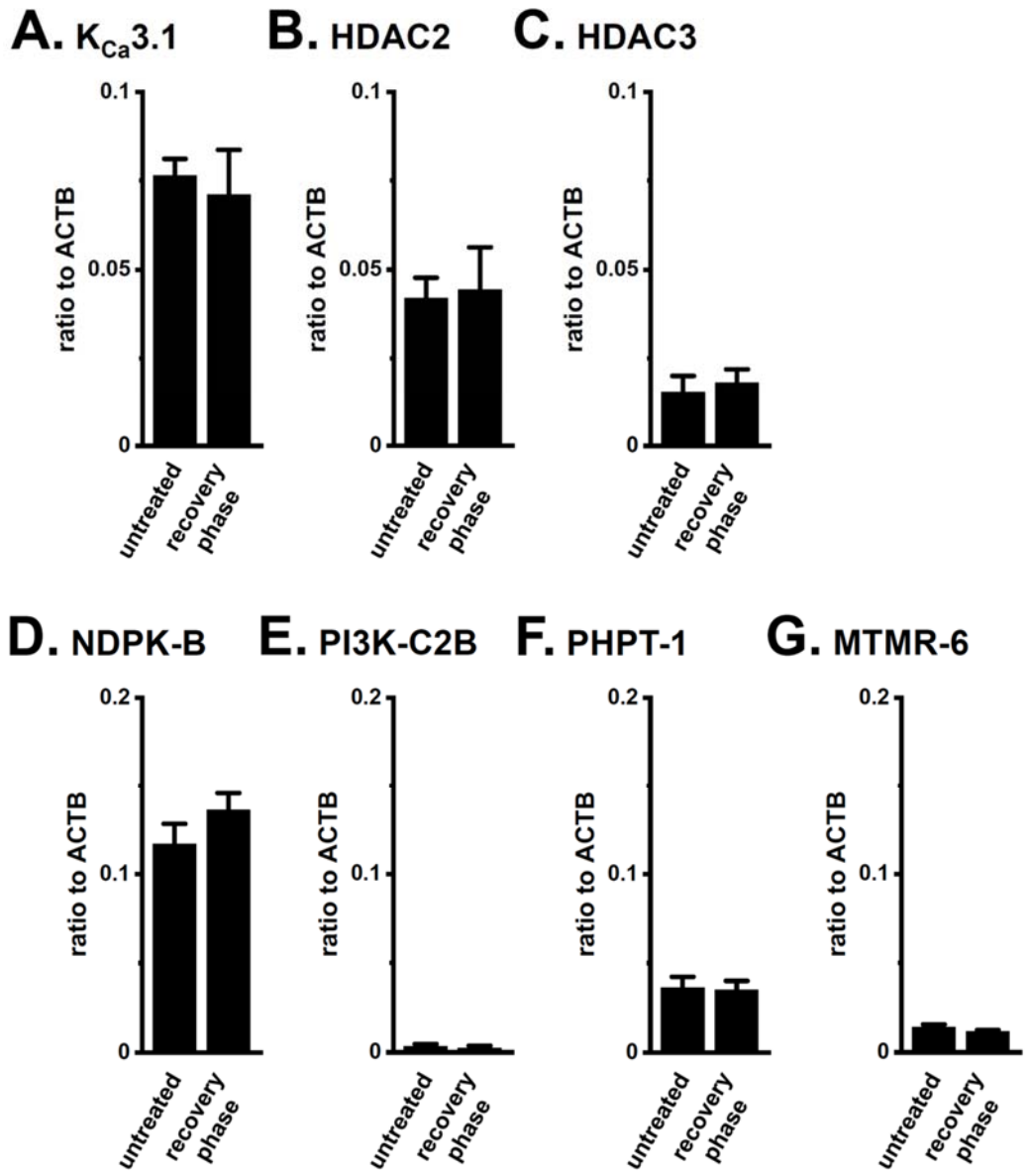

Figure S5. No changes in transcriptional expression levels of K_{Ca}3.1, HDAC2, HDAC3, and K_{Ca}3.1 modulatory β subunits in mLN $CD4^+CD25^+$ T_{reg} cells of untreated and IBD model mice in the recovery phase. A-G: Real-time PCR examinations for the transcriptional expression of K_{Ca}3.1 (A), HDAC2 (B), HDAC3 (C), NDPK-B (D), PI3K-C2B (E), PHPT-1 (F), and MTMR-6 (G) in mLN T_{reg} cells (n = 4 for each). Expression levels were expressed as a ratio to ACTB. Results are expressed as means ± SEM.

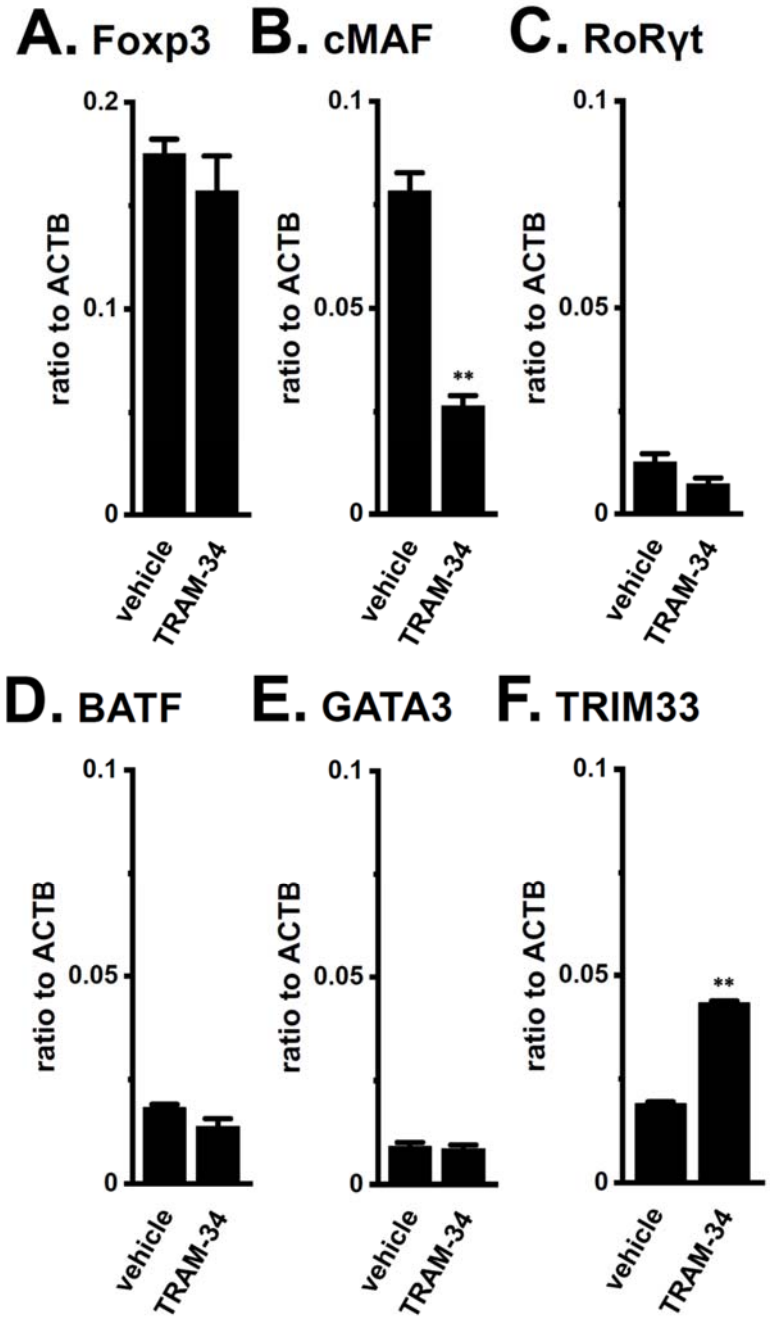

Figure S6. Expression levels of transcriptional regulators for IL-10 by the administration of TRAM-34 in mLN CD4$^+$CD25$^+$ T$_{reg}$ cells in the recovery phase in IBD model mice. A-F: Real-time PCR examinations for the transcriptional expression of Foxp3 (A), cMAF (B), RoRγt (C), BATF (D), GATA3 (E), and TRIM-33 (F) in mLN T$_{reg}$ cells in the recovery phase in IBD model mice *in vivo* administered vehicle and TRAM-34 (1 mg/kg) (n = 4 for each). Expression levels were expressed as a ratio to ACTB. Results are expressed as means ± SEM. **: $P < 0.01$ vs. vehicle-administered mice.

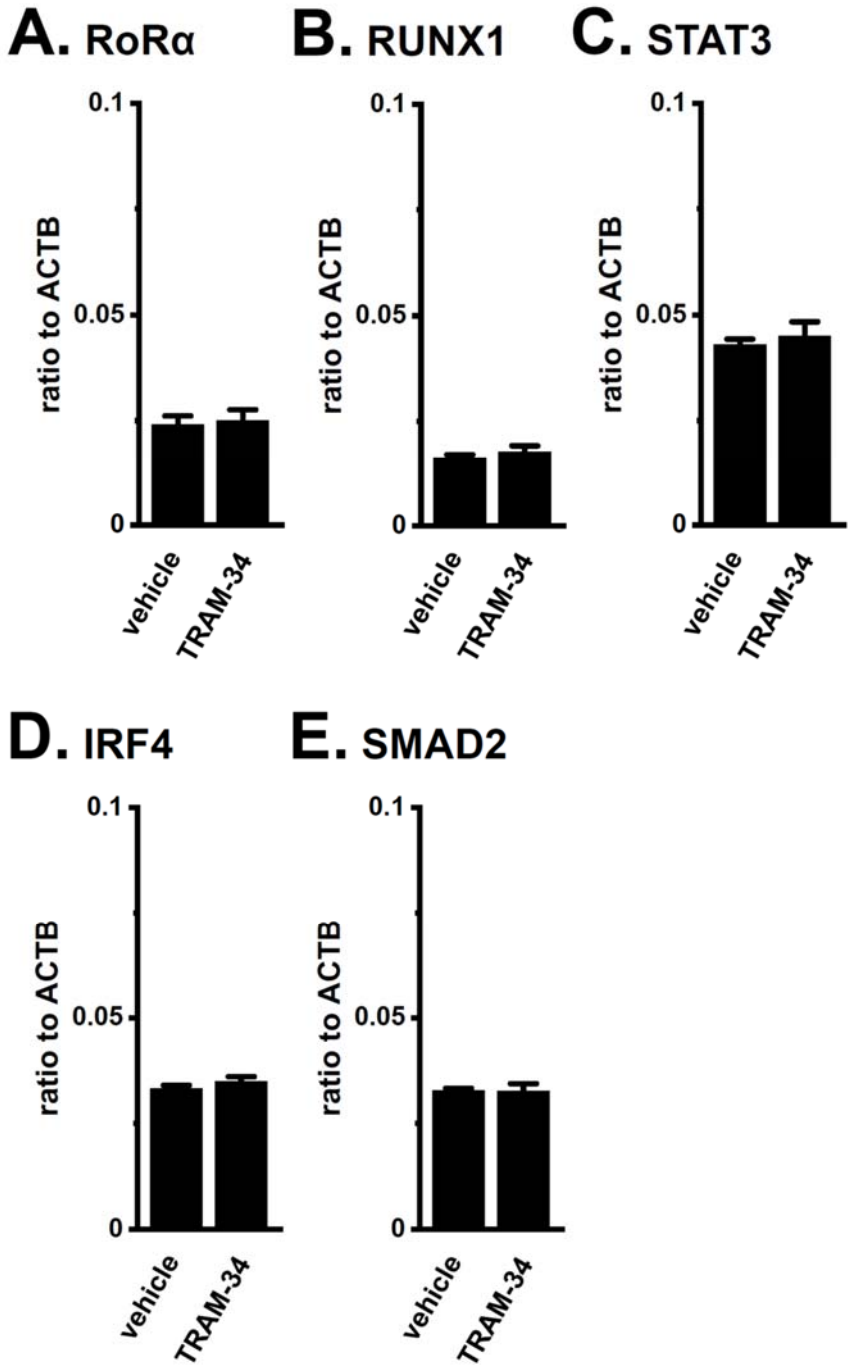

v

Figure S7. Expression levels of transcriptional regulators for IL-17A in mLN CD4$^+$CD25$^+$ T_{reg} cells in the recovery phase in IBD model mice following the administration of TRAM-34. A-E: Real-time PCR examinations for the transcriptional expression of RoRα (A), RUNX1 (B), STAT3 (C), IRF4 (D), and SMAD2 (E) in mLN T_{reg} cells in the recovery phase in IBD model mice *in vivo* administered vehicle and TRAM-34 (1 mg/kg) (n = 5 for each). Expression levels were expressed as a ratio to ACTB. Results are expressed as means ± SEM.

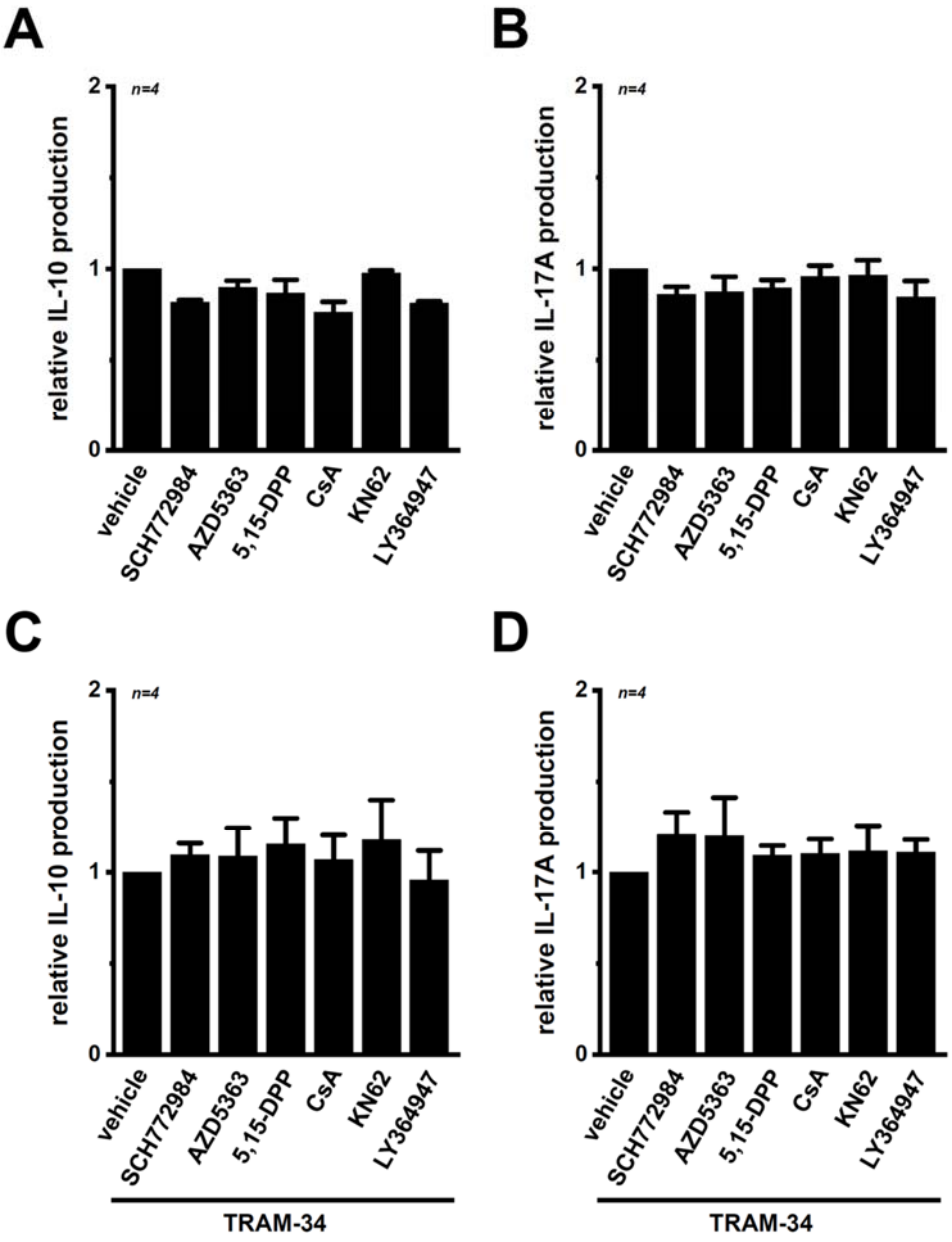

Figure S8. Effects of signaling pathway inhibitors for ERK1/2, AKT, STAT3, CN, CaMKII, and TGF-β on IL-10 and IL-17A secretion in Con-A-differentiated peripheral T_{reg} cells. A-D: Quantitative detection of IL-10 (A, C) and IL-17A (B, D) by an ELISA assay in Con-A-differentiated T_{reg} cells in the absence (A, B) and presence (C, D) of 10 μM TRAM-34 (n = 4 for each). Cells were treated with the following inhibitors for 24 hr: an ERK1/2 inhibitor (1 μM SCH772984), AKT inhibitor (5 μM AZD5363), STAT3 inhibitor (10 μM 5,15-DPP), CN inhibitor (1 μM ciclosporin A, CsA), CaMKII inhibitor (1 μM KN62), and TGF-β receptor inhibitor (10 μM LY364947). Results are expressed as means ± SEM.

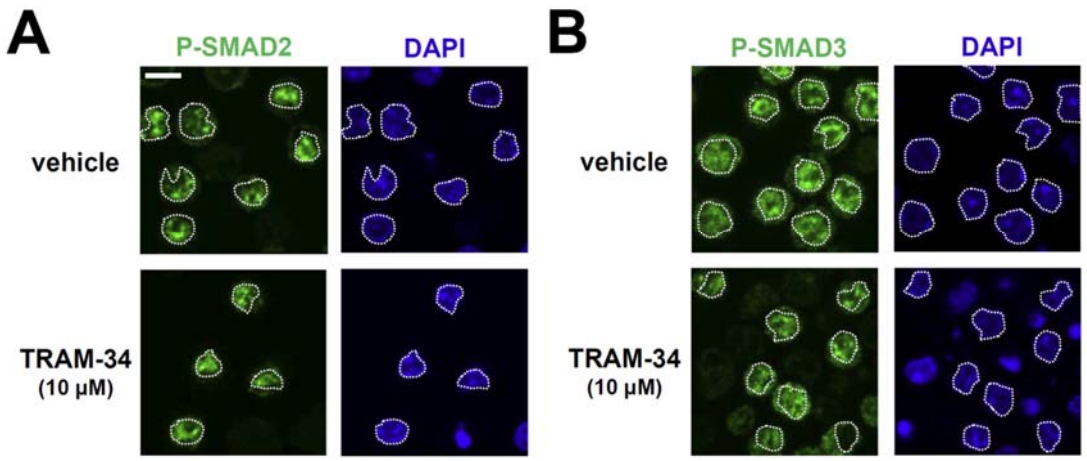

Figure S9. Effects of a treatment with 10 μM TRAM-34 on the nuclear translocation of P-Smad2 and P-Smad3 in Con-A-differentiated peripheral T_{reg} cells. A, B: Confocal fluorescent images of Alexa Fluor 488 (Green)-labeled P-SMAD2 (A, left panels) and P-SMAD3 (B, left panels) in vehicle (upper panels)- and TRAM-34 (lower panels)-treated T_{reg} cells for 24 hr. Nuclear morphologies (Blue) were shown by DAPI images (right panels of A, B). Dashed lines showed the nuclear boundary. Scale bar shows 10 μm. Similar results were obtained from four mice.